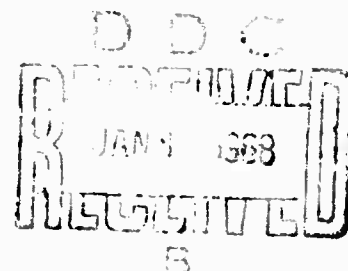MEMORANDUM
RM-5099-ARPA
NOVEMBER 1967

MID-LATITUDE VERTICAL TRANSMISSION
OF GEOMAGNETIC MICROPULSATIONS
THROUGH THE IONOSPHERE

Phyllis S. Greifinger

PREPARED FOR:

ADVANCED RESEARCH PROJECTS AGENCY

The RAND *Corporation*
SANTA MONICA · CALIFORNIA

MEMORANDUM
RM-5099-ARPA
NOVEMBER 1967

MID-LATITUDE VERTICAL TRANSMISSION
OF GEOMAGNETIC MICROPULSATIONS
THROUGH THE IONOSPHERE

Phyllis S. Greifinger

The RAND Corporation
1700 MAIN ST · SANTA MONICA · CALIFORNIA · 90406

PREFACE

This report is part of RAND's continuing efforts on the detection of high-altitude nuclear explosions. It is concerned with the ionospheric propagation of hydromagnetic waves, either natural or resulting from a nuclear burst. The results of previous propagation studies are substantially generalized and extended. The report should be of interest to people working in the following fields:

(a) Geomagnetism and related ionospheric phenomena;

(b) Geomagnetic effects of high-altitude nuclear bursts;

(c) Electromagnetic wave propagation in plasmas, particularly the ionosphere.

The author is a consultant to The RAND Corporation.

SUMMARY

In this paper we consider the two cases of a "fast" or "slow" hydromagnetic wave of unit amplitude and of extremely low frequency (below a few cps) incident on the upper ionosphere (below the F_2 electron-density maximum) at middle or high latitudes, and we study its vertical propagation through the ionosphere. From approximate solutions of the propagation equations, we obtain analytic expressions for t magnetic field at the ground, as a function of the various relevant quantities such as wave frequency, polarization of the incident wave, ionospheric ion density, ion cyclotron frequency, ion-neutral collision frequency, and the dip angle of the earth's magnetic field. The results are compared with those of previous theoretical studies for a few special cases, and with recently reported experimental observations. In both cases, the agreement is good. A few qualitative features of our results for frequencies between about .25 and 2 cps are:

(1) For middle to high latitudes, excluding the polar regions, the order of magnitude of the transmitted magnetic field is insensitive to the polarization of the incident wave.

(2) The daytime transmitted fields should be predominantly of right-handed circular polarization (in the horizontal plane) regardless of the polarization of the incident fields.

(3) The relative daytime amplitudes of the transmitted fields for the different frequencies are insensitive to changes in the ionospheric ion density, while the absolute values decrease exponentially with increasing ion density.

(4) Day-night amplitude ratios vary between about .05 and 1, depending mostly upon daytime ion density, and are insensitive to the wave frequency for frequencies above about .5 cps.

ACKNOWLEDGMENTS

CONTENTS

BLANK PAGE

I. INTRODUCTION

In this paper we will consider theoretically the transmission of extremely low-frequency (below a few cps) geomagnetic pulsations propagating vertically through the daytime ionosphere at middle and high latitudes. By the term "ionosphere" we will be referring to the region below the F_2 electron density maximum; the filtering action of the lower exosphere will not be considered here.

It is generally assumed that most of the extremely low-frequency natural fluctuations in the geomagnetic field observed at the earth's surface have their source somewhere above the ionosphere and propagate downward through the ionosphere as hydromagnetic "waves." If we are to use the ground data to make deductions concerning the amplitude, frequency of occurrence, and frequency spectra of such disturbances above the ionosphere, we need to know the transmission properties of the ionosphere itself. Since the various parameters characterizing the ionosphere vary with latitude and fluctuate with season, time of day, and sunspot conditions, it is virtually impossible to interpret ground data without at least some knowledge of the qualitative dependence of the transmitted fields on the relevant ionospheric parameters, and of the order of magnitude of the changes to be expected in the transmitted fields as these parameters undergo certain changes.

For this purpose it is very useful to obtain analytic approximations of the transmitted amplitudes as a function of the various relevant quantities such as wave frequency, polarization of the incident wave, ionospheric ion density, ion cyclotron frequency, ion-neutral collision frequency, and the dip angle of the earth's magnetic field.

The transmission properties of the ionosphere for hydromagnetic disturbances in the frequency range of interest here have been calculated for a few special cases. Greifinger and Greifinger (1965), in a paper henceforth referred to as I, obtained an analytic expression for the ionospheric transmission coefficient for polar propagation through a simple, idealized model ionosphere. Francis and Karplus (1960), and Karplus, Francis, and Dragt (1962), in two works henceforth referred to as II and III, respectively, calculated the transmitted amplitudes

of hydromagnetic waves vertically incident on the ionosphere at an altitude of 550 km for a 60-deg dip angle of the earth's magnetic field. The results of II and III were obtained by numerical integration of the relevant differential equations for a few frequencies in the range of 1 to 30 rad/sec for four sets of ionospheric parameters corresponding to day and night at minimum and maximum sunspot conditions. Wentworth (1964) used the results of III to obtain an empirical expression relating attenuation in the ionosphere to the wave frequency and to the F_2 peak-ion density. Prince and Bostick (1964) and Field and Greifinger (1965) have treated the case of vertical propagation at the equator. We will not refer again to these last two works, since the transmission characteristics of the equatorial ionosphere are quite different from those at other latitudes, and we are concerned here only with middle- and high-latitude transmission.

The main qualitative features of the results of I for daytime polar propagation are:

(1) the critical dependence of the transmitted amplitude on the polarization of the incident wave, with waves of left-handed circular polarization being evanescent in the lower ionosphere and strongly attenuated for frequencies above .1 to .5 cps (depending upon sunspot conditions), and waves of right-handed circular polarization being only slightly attenuated for frequencies less than a cps (the attenuation in this case being due to collisional absorption), and

(2) the existence of a very low-frequency transmission maximum for a wave of right-handed circular polarization. (Unfortunately, in I, the wave modes are labeled contrary to the usual convention. The electric (or magnetic) vector for the wave labeled L in I actually has right-handed circular polarization when viewed along the earth's magnetic field, and the R wave of I has left-handed circular polarization.)

The main features of the results of II and III for daytime propagation are:

(1) the strong dependence of the transmitted amplitudes on sunspot conditions,

(2) the decoupling of the fields into circularly polarized fields in the lower ionosphere, with the preferential transmission of waves of

right-handed circular polarization, regardless of the polarization of
the wave incident on the upper ionosphere, and

(3) the insensitivity of the order of magnitude of the amplitude
of the transmitted magnetic field to the polarization of the incident
wave.

For the case of nighttime transmission at frequencies below a few
cps, the results of I, II, and III show that the normal ionosphere is
essentially transparent below about 300 km; however, the transmitted
amplitudes may be affected by anomalies (such as sporadic e-layer).
Reflection from the earth, of course, affects nighttime transmission
as it does the daytime.

In this paper we extend the analyses of I, II, and III to obtain
approximate analytic expressions for the transmitted field amplitudes
of low-frequency hydromagnetic waves vertically incident on the daytime
ionosphere as a function of the relevant parameters. We give numerical
results for middle-latitude parameters obtained from the ionosphere pro-
files of Sims and Bostick (1963) under minimum and maximum sunspot con-
ditions and predict the changes if different values are employed. More
specifically, we obtain approximate expressions for the amplitude of the
transmitted daytime magnetic field at middle and high latitudes and for
its ratio to the amplitude of the transmitted nighttime field as a func-
tion of wave frequency, polarization of the incident fields, and iono-
spheric ion density. In addition, we investigate the effects on the
transmitted fields of the altitude-dependence of the ion--neutral col-
lision frequency, since this is the only relevant ionospheric parameter
which changes drastically from the bottom to the top of the ionosphere.

Our results are compared with the numerical calculations of III
and with experimental observations recently reported by Campbell (1967);
in both cases the agreement is generally good.

The main qualitative features of our results for vertical propaga-
tion of frequencies between about .25 and 2 cps at middle latitudes are:

(1) As in II and III, the order of magnitude of the transmitted
magnetic field is insensitive to the polarization of the incident wave;
changes of the latter are not likely to affect the transmitted field by
more than a factor of about 2.

(2) The amplitude of the transmitted field decreases exponentially with increasing density of ionospheric ions--by 1/e for an increased ion density of about 55 percent.

(3) The relative daytime transmitted amplitudes of the different frequencies are insensitive to changes in ion density. Thus the shape of the amplitude--frequency curve observed at the ground should be independent of season, time of day, and sunspot conditions, provided that the shape of the amplitude--frequency curve in the upper ionosphere is unchanged.

(4) The ratio of the day--night amplitude varies between .05 and 1, depending upon ion density. The frequency-dependence of this ratio is slight for frequencies above about .5 cps.

(5) The fields transmitted in the daytime should be predominantly of right-handed circular polarization (in the horizontal plane), regardless of the polarization of the incident fields.

If for polar propagation we use, instead of the short-range exponential form employed in I, a more realistic, longer-range function for the dependence of the ion-neutral collision frequency on altitude, the transmitted amplitudes become smaller than those of I, and the transmission maximum becomes both broader and flatter than that of I. Otherwise, our results for polar propagation are qualitatively similar to those of I.

II. PROPAGATION EQUATIONS

For the sake of completeness, we shall briefly review the equations derived in II governing the propagation of hydromagnetic waves in the ionosphere. Our basic assumptions are the same as those in II; the iono- sphere is motionless and flat, hydrostatic and gravitational forces may be neglected, the motion of neutral particles and the collisions between electrons and ions may be neglected, the earth's magnetic field is uni- form, the parameters describing the medium vary only in the vertical direction, and the normal to the wave is in the vertical direction. We also linearize the equations of motion, as is customary.

We shall take the positive z-direction to be vertically downward and the static magnetic field to be in the x-z plane. The electric field E and the perturbed magnetic field B may be written

$$E = (E_x, E_y, E_z) \tag{1}$$

$$B = (B_x, B_y, 0)$$

Assuming a time-dependence of the form $e^{-i\omega t}$, and neglecting the dis- placement current, we start with the wave equation

$$\vec{\nabla} \times (\vec{\nabla} \times \vec{E}) = \vec{\nabla}(\vec{\nabla} \cdot \vec{E}) - \nabla^2 \vec{E} = \frac{4\pi i \omega}{c^2} \vec{j} \tag{2}$$

where $\vec{j}$ is the current density and is related to $\vec{E}$ by

$$\vec{j} = \sigma_o \vec{e}_o (\vec{E} \cdot \vec{e}_o) + \sigma_1 [\vec{E} - \vec{e}_o (\vec{E} \cdot \vec{e}_o)] + \sigma_2 \vec{E} \times \vec{e}_o \tag{3}$$

The vector $\vec{e}_o$ is a unit vector in the direction of $\vec{B}_o$; $(e_o)_z = \cos \varphi$, and $(e_o)_x = \sin \varphi$, where φ is the complement of the dip angle. The con- ductivity components σ_o, σ_1, and σ_2 are given by

$$\sigma_0 = e^2 N_1 \left[\frac{1}{m_i(\nu_i - i\omega)} + \frac{1}{m_e(\nu_e - i\omega)} \right] \tag{4}$$

$$\sigma_1 = e^2 N_1 \left\{ \frac{\nu_i - i\omega}{m_i[(\nu_i - i\omega)^2 + \omega_i^2]} + \frac{\nu_e - i\omega}{m_e[(\nu_e - i\omega)^2 + \omega_e^2]} \right\} \tag{5}$$

$$\sigma_2 = e^2 N_1 \left\{ \frac{\omega_i}{m_i[(\nu_i - i\omega)^2 + \omega_i^2]} - \frac{\omega_e}{m_e[(\nu_e - i\omega)^2 + \omega_e^2]} \right\} \tag{6}$$

where N_1 is the volume density of ion pairs, m_i and m_e are the ion and electron masses, ν_i and ν_e are the ion and electron collision frequencies, and ω_i and ω_e are the cyclotron frequencies of ions and electrons, respectively. As in II, it is convenient to introduce the auxiliary quantities

$$\sigma_3 = \sigma_1 + \frac{\sigma_2^2}{\sigma_1} \tag{7}$$

$$\sigma_1' = \cos^2 \varphi + \frac{\sigma_1}{\sigma_0} \sin^2 \varphi \tag{8}$$

$$\sigma_3' = \cos^2 \varphi + \frac{\sigma_3}{\sigma_0} \sin^2 \varphi \tag{9}$$

The field equations for the transverse components E_x and E_y of the electric field are then given by

$$\left[\frac{d^2}{dz^2} + \frac{4\pi i \omega}{c^2} \frac{\sigma_1}{\sigma_1'} \right] E_x + \frac{4\pi i \omega}{c^2} \frac{\sigma_2 \cos \varphi}{\sigma_1'} E_y = 0 \tag{10}$$

$$\left[\frac{d^2}{dz^2} + \frac{4\pi i \omega}{c^2} \frac{\sigma_1}{\sigma_1'} \sigma_3' \right] E_y - \frac{4\pi i \omega}{c^2} \frac{\sigma_2 \cos \varphi}{\sigma_1'} E_x = 0 \tag{11}$$

The longitudinal component E_z of the electric field, which is not a dynamic variable, can be expressed in terms of E_x and E_y:

$$E_z = \frac{\sin \varphi}{\sigma_1'} \left[E_y \frac{\sigma_2}{\sigma_o} + E_x \cos \varphi \left(\frac{\sigma_1}{\sigma_o} - 1 \right) \right] \qquad (12)$$

Henceforth, we shall concern ourselves only with field components in the x-y plane.

An examination of representative height profiles of collision and cyclotron frequencies shows that, except for very small dip angles (a few degrees or less), electron collisions are negligible and

$$\sigma_1' \sim \sigma_3' \sim \cos \varphi \qquad (13)$$

Substituting Eq. (13) into Eqs. (10) and (11), and neglecting ν_e, we get

$$\left[\frac{d^2}{dz^2} + \frac{4\pi i \omega}{c^2} \frac{\sigma_1}{\cos^2 \varphi} \right] E_x + \frac{4\pi i \omega}{c^2} \frac{\sigma_2}{\cos \varphi} E_y = 0 \qquad (14)$$

$$\left[\frac{d^2}{dz^2} + \frac{4\pi i \omega}{c^2} \sigma_1 \right] E_y - \frac{4\pi i \omega}{c^2} \frac{\sigma_2}{\cos \varphi} E_x = 0 \qquad (15)$$

where

$$\frac{4\pi i \omega \, \sigma_1}{c^2} \simeq \frac{\omega_1^2}{v_a^2} \left[\frac{\omega(\omega + i\nu_1)}{\omega_1^2 + (\nu_1 - i\omega)^2} \right] \qquad (16)$$

$$\frac{4\pi i \omega \, \sigma_2}{c^2} \simeq - \frac{\omega_1^2}{v_a^2} \left(\frac{i\omega}{\omega_1} \right) \left[\frac{(\nu_1 - i\omega)^2}{(\nu_1 - i\omega)^2 + \omega_1^2} \right] \qquad (17)$$

$$V_a = \left[\frac{B_o^2}{4\pi N_1 M_1}\right]^{1/2} = \text{Alfvén speed} \tag{18}$$

One boundary condition is that the field components E_x and E_y vanish at the surface of the earth, which we treat as a perfect conductor at the low frequencies of interest here. Additional boundary conditions will be discussed later.

one real and the other imaginary, within the approximation used. Thus, the two modes are sometimes referred to as propagating (p) and evanescent (e). When viewed along the earth's magnetic field, the E (or B) vector rotates clockwise in the p-mode and counterclockwise in the e-mode. In I the p- and e-modes are unfortunately referred to as L and R modes, respectively, contrary to the usual convention. This terminological confusion results from the dependence of the sense of rotation on the direction from which the fields are viewed, and we shall henceforth use the unambiguous "p" and "e" labels for the modes.

In the Alfvén region, Eqs. (14) to (18) become

$$\left[\frac{d^2}{dz^2} + \frac{\omega^2}{v_a^2 \cos^2 \varphi \left(1 - \frac{\omega^2}{\omega_i^2}\right)}\right] E_x + \frac{i\omega}{\omega_i \cos \varphi} \frac{\omega^2}{v_a^2 \left(1 - \frac{\omega^2}{\omega_i^2}\right)} E_y \cong 0 \qquad (20)$$

$$\left[\frac{d^2}{dz^2} + \frac{\omega^2}{v_a^2 \left(1 - \frac{\omega^2}{\omega_i^2}\right)}\right] E_y - \frac{i\omega}{\omega_i \cos \varphi} \frac{\omega^2}{v_a^2 \left(1 - \frac{\omega^2}{\omega_i^2}\right)} E_x \cong 0 \qquad (21)$$

When V_a and ω_i are constant, solutions have the form $e^{\pm ikz}$, and the dispersion relationship is given by

$$\frac{v_a^2 k^2}{\omega^2} \equiv \frac{v_a^2}{v_{ph}^2} = \frac{1}{2\left(1 - \frac{\omega^2}{\omega_i^2}\right)}\left[1 + \frac{1}{\cos^2 \varphi} \pm \frac{1}{\cos^2 \varphi} \sqrt{\sin^4 \varphi + \frac{4\omega^2 \cos^2 \varphi}{\omega_i^2}}\right]$$

$$(22)$$

where

$$V_{ph} = \frac{\omega}{k} \qquad (23)$$

is the phase velocity.

III. IONOSPHERIC REGIONS AND NORMAL MODES OF RADIATION

For hydromagnetic waves in the frequency regime below a few cps, the ionosphere consists of three regions that are characterized by the relative magnitudes of ν_1, ω_1, and ω, and by cos φ (see I). In order of increasing altitude, these regions are:

(a) Hall region ($\omega < \omega_1 < \nu_1$ cos φ)

(b) Transition region ($\omega < \nu_1 < \omega_1/$cos φ)

(c) Alfvén region ($\nu_1 < \omega < \omega_1$)

The location of the "boundary" between the Alfvén and transition regions depends upon ω and upon sunspot conditions. For a given ω, the altitude of this boundary increases with the sunspot number as the result of the higher collision frequencies associated with periods of high solar activity.

The height of the upper "boundary" of the Hall region is independent of ω and only slightly dependent upon latitude at high and middle latitudes. (At very low magnetic latitudes, where cos φ is small, the Hall region becomes thin, and it vanishes near the equator.) The thickness of the Hall region also depends upon sunspot conditions, the upper boundary increasing in altitude from about 120 km at sunspot minimum to about 130 km at sunspot maximum.

The character of the propagation equations and the properties of the normal modes of the radiation are quite different in the different regions. In the Hall region, $|\sigma_1|/$cos $\varphi < |\sigma_2|$. If $|\sigma_1|/$cos φ is negligible compared to $|\sigma_2|$, Eqs. (14) to (18) become approximately

$$\frac{d^2}{dz^2}\left[E_x \mp iE_y\right] \simeq \mp \frac{\omega}{\omega_1} \frac{\omega_1^2}{v_a^2} \left[E_x \mp iE_y\right] \tag{19}$$

The two normal modes ($E_y = \pm iE_x$) are circularly polarized in the horizontal plane, and are characterized by distinct indices of refraction,

one real and the other imaginary, within the approximation used. Thus, the two modes are sometimes referred to as propagating (p) and evanescent (e). When viewed along the earth's magnetic field, the E (or B) vector rotates clockwise in the p-mode and counterclockwise in the e-mode. In I the p- and e-modes are unfortunately referred to as L and R modes, respectively, contrary to the usual convention. This terminological confusion results from the dependence of the sense of rotation on the direction from which the fields are viewed, and we shall henceforth use the unambiguous "p" and "e" labels for the modes.

In the Alfvén region, Eqs. (14) to (18) become

$$\left[\frac{d^2}{dz^2} + \frac{\omega^2}{v_a^2 \cos^2\varphi\left(1 - \frac{\omega^2}{\omega_i^2}\right)}\right] E_x + \frac{i\omega}{\omega_i \cos\varphi} \frac{\omega^2}{v_a^2\left(1 - \frac{\omega^2}{\omega_i^2}\right)} E_y \cong 0 \qquad (20)$$

$$\left[\frac{d^2}{dz^2} + \frac{\omega^2}{v_a^2\left(1 - \frac{\omega^2}{\omega_i^2}\right)}\right] E_y - \frac{i\omega}{\omega_i \cos\varphi} \frac{\omega^2}{v_a^2\left(1 - \frac{\omega^2}{\omega_i^2}\right)} E_x \cong 0 \qquad (21)$$

When V_a and ω_i are constant, solutions have the form $e^{\pm ikz}$, and the dispersion relationship is given by

$$\frac{v_a^2 k^2}{\omega^2} \equiv \frac{v_a^2}{v_{ph}^2} = \frac{1}{2\left(1 - \frac{\omega^2}{\omega_i^2}\right)}\left[1 + \frac{1}{\cos^2\varphi} \pm \frac{1}{\cos^2\varphi}\sqrt{\sin^4\varphi + \frac{4\omega^2\cos^2\varphi}{\omega_i^2}}\right]$$

$$(22)$$

where

$$V_{ph} = \frac{\omega}{k} \qquad (23)$$

is the phase velocity.

Thus, Eqs. (30) and (31) provide a smooth transition from linearly polarized to circularly polarized normal modes as φ decreases from about $\sqrt{2\omega/\omega_i}$ to 0.

The nomenclature of the two modes in the Alfvén region is a source of as much confusion as the nomenclature of the modes in the Hall region. In II and III, the fast and slow waves are referred to as "ordinary" and "extraordinary," respectively. Other authors reverse this nomenclature, referring to the fast wave as "extraordinary." Other terms commonly used for the slow wave are "Alfvén mode," "L-mode," and "ion cyclotron wave," (the last two referring to the wave properties for parallel propagation). The fast wave is sometimes described as "R-mode" or "isotropic;" the latter term refers to the lack of dependence of its phase velocity on φ, and the former to its polarization for parallel propagation. Needless to say, it would be helpful if a standard nomenclature were adopted.

We have seen that the waves can be described in terms of (nearly) uncoupled normal modes in idealized Alfvén and Hall regions. The polarization of the two modes in the Alfvén region is elliptical, the two ellipses becoming mutually perpendicular straight lines when $\varphi \gg \sqrt{2\omega/\omega_i}$ and circles when $\varphi \ll \sqrt{2\omega/\omega_i}$. In the Hall region, the normal modes are circularly polarized in the horizontal plane.

The transition from one pair of normal modes in the Alfvén region to another pair in the Hall region takes place in the transition region, where the waves are coupled because of collisions. This coupling of modes is an important property of the daytime ionosphere, and leads to changes in the polarization of the radiation as it passes through the ionosphere.

An exception occurs when the wave propagates parallel to the magnetic field. For $\varphi = 0$, and for a model ionosphere in which all parameters vary only in the vertical direction, the two circularly polarized normal modes remain uncoupled as the radiation descends vertically from the Alfvén region to the Hall region. The fast mode of the Alfvén region becomes the propagating mode of the Hall region, and the slow mode of the Alfvén region becomes the evanescent mode of the Hall region. This was the case in I, where polar propagation ($\varphi = 0$) was considered.

When $\varphi \gg \sqrt{2\omega/\omega_1}$, the radiation in the Hall region consists of a mixture of p and e modes, regardless of the polarization of the incident wave. The extent to which the transmitted fields depend upon the wave mode of the incident radiation will be discussed later.

IV. PHYSICAL MODEL

In order to find analytic solutions of the wave equation, we need to establish the functional dependence of the parameters ω_i, V_a, and ν_i on z.

According to the profiles of Sims and Bostick (1963), ω_i varies little with altitude in the ionosphere, although it is latitude-dependent. For each latitude considered, we will assume ω_i to be independent of z.

The Alfvén speed V_a depends upon latitude, time of day, sunspot conditions, and altitude. When considered as a function of 'ncreasing altitude from the surface of the earth, V_a decreases abruptly at an altitude of about 100 km. We refer to 100 km as the "bottom" of the ionosphere, since the region below 100 km is characterized by values of V_a so large that the medium behaves like a vacuum for the frequencies of interest here. For altitudes above 100 km but below the F_2 minimum of the Alfvén speed, V_a decreases with altitude, the total decrease from the bottom to the top of the ionosphere being about a factor of 2 or 3, depending upon sunspot conditions. In the Hall region the variations are slight, and V_a can be taken as constant. Similarly, in the Alfvén region V_a decreases slowly up to the F_2 minimum and can be regarded as constant. In the transition region, we shall see that V_a enters the equations only as part of the factor ν_i/V_a^2; thus we will not need to be concerned with V_a itself.

The ion-neutral collision frequency ν_i changes by a few orders of magnitude from the lower to the upper portions of the ionosphere, decreasing from several thousand collisions/sec at 100 km to a value between about .1 and 1 collision/sec, depending upon sunspot conditions, at about 300 km. We shall be concerned with the functional dependence on z of the quantity ν_i/V_a^2 in the transition region; this quantity is usually expressed in terms of a scale height ζ:

$$\frac{\nu_i}{V_a^2} = \frac{\omega_i}{(V_a^2)_{z=0}} \exp\left[\int_0^z \frac{dz}{\zeta(z)}\right] \tag{32}$$

where we have taken $z = 0$ to be the altitude for which $\nu_i = \omega_i$. The scale height ζ increases with altitude from the bottom to the top of ionosphere, varying from a few km near the bottom to about 100 km near the top. Since the height of the upper boundary of the transition region is frequency-dependent, extending to nearly the top of the ionosphere for the lowest frequencies considered, we need an approximation of $\zeta(z)$ that is applicable to the entire ionosphere above the Hall region.

In I, ζ was assumed to be constant and equal to its value ζ_0 at $z = 0$. This, of course, is the simplest approximation, but since it greatly underestimates the collision frequencies at high altitudes, it leads to an overestimate of the amplitude of the transmitted field for those frequencies at which the transition region extends a distance greater than about $2\zeta_0$ above $z = 0$. For frequencies high enough so that the thickness of the transition region is of order $2\zeta_0$ (or less), ζ can be replaced by ζ_0.

The simplest way to approximate ζ to take account of its increase with altitude is to assume it to be a linear function of z. This leads to a power law, rather than an exponential dependence of ν_i/V_a^2 on altitude:

$$\frac{\nu_i}{V_a^2} \approx \frac{\omega_i}{(V_a^2)_{z=0}} \frac{1}{\left[1 - \dfrac{z}{P\zeta_0}\right]^P} \tag{33}$$

Equation (33) provides a reasonably good approximation to ν_i/V_a^2 when the power P is equal to about 2 and ζ_0 is about 10 km at sunspot minimum and 15 km at sunspot maximum. This can be seen from Fig. 1, where we have plotted Eq. (33) together with the values of ν_i/V_a^2 given by Sims and Bostick (1963). The latitude-dependence of the functional form of ν_i/V_a^2 is slight; Eq. (33) is equally applicable at all latitudes considered here. We shall use Eq. (33) with $P = 2$ and compare the results with those obtained by using a constant value of ζ, as in I.

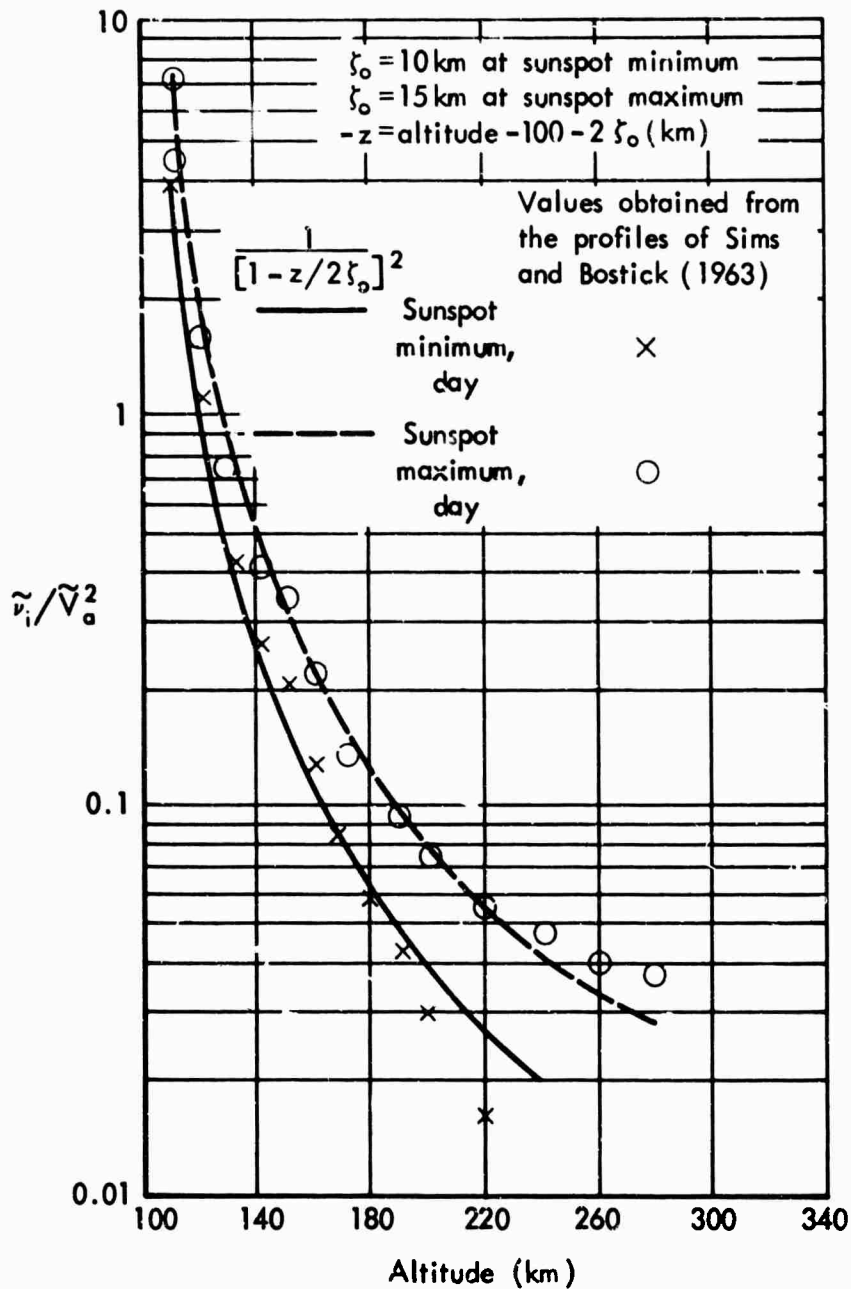Fig. 1 -- The ion-neutral collision frequency divided by the square of the Alfvé speed, normaliz~d to unity at the altitude at which the ion-neutral collision frequency equals the ion cyclotron frequency ω_i. The data points are from the ionospheric profiles of Sims and Bostick (1963) for a magnetic dip angle of 74°. The solid curves are the empirical fits to the data points given by Eq. (33) when P = 2.

V. BOUNDARY CONDITIONS AND TRANSMISSION MATRIX

Before we find solutions to the propagation equations, we must
specify the boundary conditions. The vanishing of the electric field
at the surface of the earth gives as one boundary condition

$$\left(\frac{dE_{x,y}}{dz}\right)_{z_1} = -\frac{1}{h} E_{x,y}(z_1) \tag{34}$$

where z_1 is the coordinate of the bottom of the ionosphere and h is the
thickness of the vacuum region (100 km).

The choice of the additional boundary conditions is rather arbi-
trary, since we are disregarding the source of the radiation. Most
source models currently assume that the radiation impinges on the iono-
sphere either as a slow wave arriving from a source in the magnetosphere
or as a fast wave that has arrived from another latitude via an iono-
spheric duct located near the F_2 electron-density maximum. Thus for
convenience we shall consider the two cases where the incident wave is
either a pure slow (S) or a pure fast (F) wave.

In order to translate this assumption into a specific boundary con-
dition for the incident fields, let us examine the asymptotic form of
the electric and magnetic field components in the Alfvén region. In
this region the components of the electric field satisfy Eqs. (20) and
(21). We will assume that $|\omega/\omega_1| \ll 1$, that $|(\omega/\omega_1)E_x|$ is negligible
compared to $|E_y|$, and that $|(\omega/\omega_1)E_y|$ is negligible compared to $|E_x|$.
Equations (20) and (21) then become uncoupled into the two equations

$$\left(\frac{d^2}{dz^2} + \frac{\omega^2}{v_a^2 \cos\varphi}\right) E_x = 0 \tag{35}$$

$$\left(\frac{d^2}{dz^2} + \frac{\omega^2}{v_a^2}\right) E_y = 0 \tag{36}$$

From the induction equation, we know that B_y satisfies Eq. (35) and B_x satisfies Eq. (36). Therefore, the field components in the Alfvén region can be written in the form

$$B_x = A_x e^{ik_x z} + (r_{xx} A_x + r_{xy} A_y) e^{-ik_x z} \tag{37}$$

$$B_y = A_y e^{ik_y z} + (r_{yy} A_y + r_{yx} A_x) e^{-ik_y z} \tag{38}$$

$$E_y = -\frac{1}{c}\left[A_x e^{ik_x z} - (r_{xx} A_x + r_{xy} A_y) e^{-ik_x z} \right] \tag{39}$$

$$E_x = \frac{\cos \varphi}{c}\left[A_y e^{ik_y z} + (r_{yy} A_y + r_{yx} A_x) e^{-ik_y z} \right] \tag{40}$$

where

$$k_x \equiv \frac{\omega}{V_a} \tag{41}$$

$$k_y \equiv \frac{\omega}{V_a \cos \varphi} \tag{42}$$

We have expressed the reflected wave in terms of the elements r_{xx}, r_{xy},..., of a 2-by-2 matrix. The presence of nonvanishing off-diagonal elements r_{xy} and r_{yx} is a consequence of coupling below the Alfvén region. A particular field component may be present in the reflected wave even if it is absent from the incident wave. (Thus B_x contains a term proportional to A_y, etc.)

The reflection matrix is unknown and can be determined only after Eqs. (14) and (15) are solved. In order to apply the boundary condition that specifies the mode of the incident wave in the Alfvén region, it is convenient to eliminate the unknown reflection terms from Eqs. (37) to (40) and to relate the field components and their derivatives

to specified components of the incident field. From Eqs. (37) to (40) we get

$$E_x + \frac{\cos \varphi}{\frac{i\omega}{V_a}} \frac{dE_x}{dz} = \frac{2}{c} \cos \varphi (B_y)_{inc} \tag{43}$$

$$E_y + \frac{1}{\frac{i\omega}{V_a}} \frac{dE_y}{dz} = -\frac{2}{c} (B_x)_{inc} \tag{44}$$

where

$$(B_x)_{inc} \equiv A_x e^{ik_x z} \tag{45}$$

$$(B_y)_{inc} \equiv A_y e^{ik_y z} \tag{46}$$

The F or S character of the incident wave determines the polarization of the incident fields and gives the relative values of A_x and A_y as a function of φ. The magnitudes of A_x and A_y will be chosen so as to normalize the incident magnetic vector to unit magnitude, i.e.,

$$|A_x|^2 + |A_y|^2 = 1 \tag{47}$$

Thus, combining Eqs. (24) to (31) with Eqs. (39), (40), and (47), we obtain:

Incident Fast Wave

$$A_y = 0, \quad A_x = 1 \quad \text{for} \quad \varphi > \sqrt{\frac{2\omega}{\omega_i}} \tag{48}$$

$$A_y \simeq iA_x\left(1 - \frac{\varphi^2}{\frac{2\omega}{\omega_1}}\right) = i\left(1 - \frac{\varphi^2}{\frac{2\omega}{\omega_1}}\right)\left[\left(1 - \frac{\varphi^2}{\frac{2\omega}{\omega_1}}\right)^2 + 1\right]^{-1/2} \quad \text{for} \quad \varphi < \sqrt{\frac{2\omega}{\omega_1}}$$

$$\tag{49}$$

$$A_y = iA_x = \frac{1}{\sqrt{2}} \quad \text{for} \quad \varphi = 0 \tag{50}$$

Incident Slow Wave

$$A_y = 1, \quad A_x = 0 \quad \text{for} \quad \varphi > \sqrt{\frac{2\omega}{\omega_1}} \tag{51}$$

$$A_x \simeq iA_y\left(1 - \frac{\varphi^2}{\frac{2\omega}{\omega_1}}\right) = i\left(1 - \frac{\varphi^2}{\frac{2\omega}{\omega_1}}\right)\left[\left(1 - \frac{\varphi^2}{\frac{2\omega}{\omega_1}}\right)^2 + 1\right]^{-1/2} \quad \text{for} \quad \varphi < \sqrt{\frac{2\omega}{\omega_1}}$$

$$\tag{52}$$

$$A_x = iA_y = \frac{1}{\sqrt{2}} \quad \text{for} \quad \varphi = 0 \tag{53}$$

Although Eqs. (50) and (53) are the limits of Eqs. (49) and (52), respectively, as $\varphi \to 0$, it is useful to consider parallel propagation separately, since it is an important special case in magnetohydrodynamic-wave theory.

Thus Eqs. (43) to (46), in conjunction with Eqs. (48) to (53), constitute our boundary conditions in the Alfvén region.

The transmitted fields are most conveniently described in terms of circularly polarized fields, regardless of the polarization of the incident fields, because of the effect of the Hall region on the radiation. Following III, we define a magnetic transmission matrix T which relates the magnetic field at the ground to the incident field:

$$\mathcal{B}_{Ground} \equiv [B_x - iB_y]_{Ground}$$

$$= \sqrt{2} \ [T_x(\omega,\varphi)(B_x)_{inc} + T_y(\omega,\varphi)(B_y)_{inc}] \tag{54}$$

For positive frequencies, the matrix T describes the transmitted p-mode, and for negative frequencies, the transmitted e-mode. The individual field components B_x and B_y and the total field magnitude $|B|$ at the ground are related to $\mathcal{B}_{Ground}$ by

$$(2B_x)_{Ground} = \mathcal{B}_{Ground}(\omega) + \mathcal{B}_{Ground}^*(-\omega) \tag{55}$$

$$(2B_y)_{Ground} = i[\mathcal{B}_{Ground}(\omega) - \mathcal{B}_{Ground}^*(-\omega)] \tag{56}$$

$$|B|_{Ground} = \left[\frac{|\mathcal{B}(\omega)|^2 + |\mathcal{B}^*(-\omega)|^2}{2} \right]^{1/2}_{Ground} \tag{57}$$

Therefore, if $T_x(\omega,\varphi)$ and $T_y(\omega,\varphi)$ are determined we can determine the transmitted magnetic field for any A_x and A_y, and it would seem unnecessary to apply any restrictions such as Eqs. (48) to (53) to the values of A_x and A_y.

However, when $\varphi \gg \sqrt{2\omega/\omega_i}$, we will see that the methods of approximation to be used in solving the equations will rely on the assumption that either A_x or A_y vanishes, so that we will be calculating the values of T_x and T_y under these conditions. The transmitted magnetic field under other conditions of polarization of the incident radiation can then only be deduced by means of an "educated guess." For example, if the incident radiation is unpolarized, it would seem reasonable to assume that the transmitted magnetic field would be approximately equal to the average of the two values that result from the condition that either A_x or A_y is zero.

We will see that $|T_x|$ and $|T_y|$ will fortunately be of the same order of magnitude for middle latitudes, so that the transmitted field

magnitudes will not be particularly sensitive to the polarization of
the incident radiction.

When φ is small (high magnetic latitudes), the propagation equations
become independent of φ, and $|T_x|$ and $|T_y|$ become equal. In this case,
we can indeed find the transmitted magnetic field for arbitrary A_x and
A_y, and can dispense with the restriction that these quantities satisfy
the conditions appropriate to an incident F- or S-wave. However, since
in some models it well may be that the source generates waves of a
given mode, such a boundary condition still appears sensible.

VI. APPROX ATIONS AND SOLUTIONS

To solve our equations, let us first rewrite Eqs. (14) to (17) in terms of dimensionless variables (denoted by a tilde) with ω_i, V_s, and V_a/ω_i at $z = 0$ as the units of frequency, speed, and length, respectively.

$$\left[\frac{d^2}{d\tilde{z}^2} + \frac{\tilde{\omega}^2 + i\tilde{\omega}\tilde{\nu}_1}{\tilde{V}_a^2 \cos^2 \varphi(1 + \tilde{\nu}_1^2)}\right]E_x - \frac{i\tilde{\omega}\tilde{\nu}_1^2}{\tilde{V}_a^2 \cos \varphi(1 + \tilde{\nu}_1^2)} E_y = 0 \qquad (58)$$

$$\left[\frac{d^2}{d\tilde{z}^2} + \frac{\tilde{\omega}^2 + i\tilde{\omega}\nu_1}{\tilde{V}_a^2(1 + \tilde{\nu}_1^2)}\right]E_y + \frac{i\tilde{\omega}\tilde{\nu}_1^2}{\tilde{V}_a^2 \cos \varphi(1 + \tilde{\nu}_1^2)} E_x = 0 \qquad (59)$$

When $\varphi < \sqrt{2\tilde{\omega}}$, we can replace $\cos \varphi$ by 1, since we are neglecting terms of order $\tilde{\omega}$ compared to `, and thus, as in I, Eqs. (58) and (59) can be combined into one equat: for the variable $(E_x - iE_y)$:

$$\left[\frac{d^2}{d\tilde{z}^2} + q_o^2\right]\mathcal{E} = 0 \qquad (60)$$

where

$$q_o^2 = \frac{\tilde{\omega}^2 + i\tilde{\omega}\dfrac{\tilde{\nu}_1}{\tilde{V}_a^2}}{\left(1 + \dfrac{i\tilde{\nu}_1}{\tilde{V}_a^2}\right)} \qquad (61)$$

and

$$\mathcal{E} \equiv E_x - iE_y \qquad (62)$$

For $\varphi > \sqrt{2\tilde{\omega}}$, we can also write an equation for $\mathcal{E}$ in either of two identical forms

$$\left[\frac{d^2}{d\tilde{z}^2} + q_{x,y}^2(\tilde{z})\right]\mathcal{E} = Q_{x,y}(\tilde{z}) \tag{63}$$

where

$$q_x^2 = \frac{\tilde{\omega}^2 + i\tilde{\omega}\tilde{\nu}_1}{\tilde{V}_a^2\left(1 + \frac{i\tilde{\nu}_1}{\tilde{V}_a^2}\cos\varphi\right)} \tag{64}$$

$$q_y^2 = \frac{\tilde{\omega}^2 + i\tilde{\omega}\tilde{\nu}_1}{\tilde{V}_a^2\cos^2\varphi\left(1 + \frac{i\tilde{\nu}_1}{\tilde{V}_a^2\cos\varphi}\right)} \tag{65}$$

$$Q_x(\tilde{z}) = \frac{\sin^2\varphi}{(1 + \tilde{\nu}_1^2)\cos^2\varphi}(\tilde{\nu}_1\cos\varphi\, E_y - E_x)\frac{i\tilde{\omega}\tilde{\nu}_1}{\tilde{V}_a^2\left(1 + \frac{i\tilde{\nu}_1}{\tilde{V}_a^2}\cos\varphi\right)} \tag{66}$$

$$Q_y(\tilde{z}) = \frac{i\sin^2\varphi}{1 + \tilde{\nu}_1^2}\left(E_y + \frac{\tilde{\nu}_1 E_x}{\cos\varphi}\right)\frac{i\tilde{\omega}\tilde{\nu}_1}{\tilde{V}_a^2\cos^2\varphi\left(1 + \frac{i\tilde{\nu}_1}{\tilde{V}_a^2\cos\varphi}\right)} \tag{67}$$

For convenience of solution, we choose the subscript x or y in Eq. (63) according to the boundary conditions on the incident wave (the subscript x for $A_x = 1$, $A_y = 0$, and y for $A_y = 1$, $A_x = 0$). In the limit as $\varphi \to 0$, $q_{x,y} \to q_c$ and $Q_{x,y} \to 0$, so that Eq. (63) reduces to Eq. (60).

The magnitude of the inhomogeneous term $Q_{x,y}$ is small relative to $|q^2\mathcal{E}|$ in the Hall region and in the upper transition and lower Alfvén regions. The magnitude of Q relative to $|q^2\mathcal{E}|$ is largest near $z = 0(\tilde{\nu} \approx 1)$, where

$$|Q_{x,y}| \sim \sin^2 \varphi |q_{x,y}^2 \mathcal{E}| \tag{68}$$

At middle and (especially) at high latitudes, $\sin^2 \varphi$ is small. (For example, at an intermediate magnetic latitude of about 40°, $\sin^2 \varphi \approx .25$). Therefore $Q_{x,y}(\tilde{z})$ represents a small perturbation extending over a small region near $z = 0$, and in view of the approximate nature of the analytic representation of ν_1/V_a^2 which we shall employ, it seems pointless to retain $Q_{x,y}(\tilde{z})$ in Eq. (63).

If we neglect $Q_{x,y}(\tilde{z})$, Eq. (63) then becomes a homogeneous equation of the same form as Eq. (60):

$$\frac{d^2 \mathcal{E}}{d\tilde{z}^2} + q_{x,y}^2 \mathcal{E} = 0 \tag{69}$$

To solve Eq. (69) it is necessary to have an analytic approximation for the quantity $\tilde{\nu}_1/\tilde{V}_a^2$ contained in $q_{x,y}^2$. To study the sensitivity of the results to different assumptions, we shall consider both a short-range exponential dependence on altitude (as in I)

$$\frac{\tilde{\nu}_1}{\tilde{V}_a^2} = e^{z/\zeta_o} \tag{70}$$

and a long-range, inverse-square dependence

$$\frac{\tilde{\nu}_1}{\tilde{V}_a^2} = \frac{1}{\left(1 - \frac{z}{2\zeta_o}\right)^2} \qquad z > 2\zeta_o \approx z_1 \tag{71}$$

It is necessary to find solutions of Eq. (69) for the range of altitudes $\tilde{z}_1 \geq \tilde{z} \geq \tilde{z}_o(\omega)$ [where $\tilde{z}_o(\tilde{\omega})$ lies in the lower Alfvén region near the altitude at which $\nu_1 \sim \omega$] over which collisions are important.

SOLUTIONS FOR VERY SMALL ω

In the limit as $\omega \to 0$, $\mathcal{E}$ becomes a linear function of $\tilde{z}$:

$$\mathcal{E} \to \frac{2\tilde{k}_{x,y}\tilde{h}}{\tilde{c}}\left[\frac{1 + \frac{\tilde{z}_1 - \tilde{z}}{\tilde{h}}}{1 - i\tilde{k}_{x,y}(\tilde{h} + \tilde{z}_1 - \tilde{z}_o)}\right]\left[B_x - iB_y \cos \varphi\right]_{inc} \tag{72}$$

For small but finite $\tilde{\omega}$, $\mathcal{E}$ will be a nearly linear function of $\tilde{z}$. To obtain the next approximation, let us write Eq. (69) as an integral equation:

$$\mathcal{E}(\tilde{z}) = \frac{2\tilde{k}_{x,y}\tilde{h}}{\tilde{c}}\left[\frac{1 + \frac{\tilde{z}_1 - \tilde{z}}{\tilde{h}}}{1 - i\tilde{k}_{x,y}(\tilde{h} + \tilde{z}_1 - \tilde{z}_o)}\right]\left[B_x - iB_y \cos \varphi\right]_{inc}$$

$$+ \int_{\tilde{z}_o}^{\tilde{z}_1} G(\tilde{z},\tilde{z}')q_{x,y}^2(\tilde{z}')\mathcal{E}(\tilde{z}')d\tilde{z}' \tag{73}$$

where the Green function $G(\tilde{z},\tilde{z}')$ is given by

$$G(\tilde{z},\tilde{z}') = \frac{\tilde{h}U_1(\tilde{z})U_2(\tilde{z}')}{1 - i\tilde{k}_{x,y}\tilde{h}\left(1 + \frac{\tilde{z}_1 - \tilde{z}_o}{\tilde{h}}\right)} \qquad \tilde{z}_1 \geq \tilde{z} \geq \tilde{z}'$$

$$= \frac{\tilde{h}U_2(\tilde{z})U_1(\tilde{z}')}{1 - i\tilde{k}_{x,y}\tilde{h}\left(1 + \frac{\tilde{z}_1 - \tilde{z}_o}{\tilde{h}}\right)} \qquad \tilde{z}_o \leq \tilde{z} \leq \tilde{z}' \tag{74}$$

where

$$U_1(\tilde{z}) = 1 + \frac{\tilde{z}_1 - \tilde{z}}{\tilde{h}} \tag{75}$$

$$U_2(\tilde{z}) = 1 - i\tilde{k}(\tilde{z} - \tilde{z}_o) \tag{76}$$

When $|\tilde{\omega}|$ is so small that $|\tilde{\omega}\tilde{z}_0(\tilde{\omega})| < 1$, the integral can be estimated easily by replacing $U_2(\tilde{z}')$ by 1 and $\mathcal{E}(\tilde{z}')$ by a linear function of $\tilde{z}'$, which we write in the form

$$\mathcal{E}(\tilde{z}') = \mathcal{E}(\tilde{z}_1)\left(1 + \frac{\tilde{z}_1 - \tilde{z}'}{\tilde{h}}\right) \tag{77}$$

Solving Eq. (73) for $\mathcal{E}(\tilde{z}_1)$, we obtain

$$\mathcal{E}(\tilde{z}_1) \simeq \frac{\dfrac{2\tilde{k}_{x,y}\tilde{h}}{\mathcal{E}}[B_x - iB_y \cos \varphi]_{inc}}{1 - \tilde{h}\displaystyle\int_{\tilde{z}_0}^{\tilde{z}_1}\left(1 + \frac{\tilde{z}_1 - \tilde{z}}{\tilde{h}}\right)q_{x,y}^2(\tilde{z})d\tilde{z}} \tag{78}$$

The integration is trivial for either the power-law or exponential form of v_i/V_a^2. From $\mathcal{E}(\tilde{z}_1)$ we can obtain $(\mathcal{B})_{Ground}$ by applying the induction equation at the earth:

$$(\mathcal{B})_{Ground} = -\frac{\tilde{c}}{\tilde{\omega}}\left(\frac{d\mathcal{E}}{d\tilde{z}}\right)_{Ground} = \frac{\tilde{c}}{\tilde{\omega}\tilde{h}}\mathcal{E}(\tilde{z}_1) \tag{79}$$

From $(\mathcal{B})_{Ground}$ and Eq. (54), we can then find the magnetic transmission matrix T, the results for which are as follows for the two different forms of v_i/V_a^2:

When

$$\text{(a)} \qquad \frac{\tilde{v}_i}{\tilde{v}_a^2} = e^{z/\zeta_0}$$

$$T_x = iT_y = \frac{\sqrt{2}}{1 - \left(1.1\dfrac{\tilde{\omega}\tilde{h}\tilde{z}_1}{\cos \varphi}\right)(1 + i\gamma_1)} \tag{80}$$

where

$$\gamma_1 = \frac{\pi}{2} \frac{\zeta_o}{z_1} \tag{81}$$

$$\approx .7 \text{ for sunspot minimum}$$

$$\approx .8 \text{ for sunspot maximum}$$

The magnetic transmission coefficient of I reduces to Eq. (80) in the limit $|\sqrt{\tilde{\omega}}\tilde{z}_1| \ll 1$.

When

(b)

$$\frac{\tilde{\nu}_i}{\tilde{\nu}_a^2} = \frac{1}{\left(1 - \frac{z}{2\zeta_o}\right)^2}$$

$$T_x = \frac{\sqrt{2}}{1 - \dfrac{2.5\,\zeta_o\,\tilde{\omega}\tilde{h}}{(\cos\varphi)^{1/2}}\,[1 + i\gamma_2(\omega)]} \tag{82}$$

$$T_\nu = \frac{-\sqrt{2}i}{1 - \dfrac{2.5\,\zeta_o\,\tilde{\omega}\tilde{h}}{(\cos\varphi)^{3/2}}\,[1 + i\gamma_2(\omega)]} \tag{83}$$

where

$$\gamma_2 = .9\left\{1 + .09\left[\ell n(2.5\,\tilde{\zeta}_o\tilde{h}) + \ell n\,\frac{1}{2.5\,|\tilde{\omega}|\,\zeta_o\tilde{h}}\right]\right\} \tag{84}$$

$$\approx 1.35\left(1 + .07\,\ell n\,\frac{1}{2.5\,|\tilde{\omega}|\,\zeta_o\tilde{h}}\right) \text{ for sunspot minimum}$$

$$\approx 1.45\left(1 + .06\,\ell n\,\frac{1}{2.5\,|\tilde{\omega}|\,\zeta_o\tilde{h}}\right) \text{ for sunspot maximum}$$

Equations (82) and (83) have the same form as Eq. (80). Further-more, since 2.5 $\tilde{\zeta}_o$ and 1.1 $\tilde{z}_1$ are nearly equal, the major difference between the transmission matrices for the two forms of ν_1/V_a^2 lies in the difference in the numerical value of γ. This parameter is a mea-sure of the ratio of the effective size of the transition region to that of the Hall region. The significance of its magnitude can be seen by examining $|T_{x,y}|$. To compare the two forms of ν_1/V_a^2, we shall con-sider $\cos \varphi \simeq 1$ (high magnetic latitude), and replace 1.1 $\widetilde{\omega h}\tilde{z}_1$ of Eq. (80) by the essentially equivalent parameter 2.5 $\widetilde{\omega h}\tilde{\zeta}_o$. The magnitudes of $T_{x,y}$ in both cases can then be written as

$$|T_x| \simeq |T_y| \simeq \sqrt{2}\left[(1 + \gamma^2)\left(2.5\,\widetilde{\omega h}\tilde{\zeta}_o - \frac{1}{1 + \gamma^2}\right)^2 + \frac{\gamma^2}{1 + \gamma^2}\right]^{-1/2} \quad (85)$$

where

$$\gamma = \gamma_1 \quad \text{when} \quad \frac{\tilde{\nu}_1}{\tilde{V}_a^2} = e^{z/\zeta_o}$$

$$(86)$$

$$\gamma = \gamma_2 \quad \text{when} \quad \frac{\tilde{\nu}_1}{\tilde{V}_a^2} = \frac{1}{\left(1 - \frac{z}{2\zeta_o}\right)^2}$$

For positive ω (transmitted p-mode), $|T_{x,y}|$ has a maximum whose frequency and shape depend upon γ. For small γ, the peak is high and narrow, and gives rise to resonance phenomena. For larger values of γ, the frequency of the maximum is shifted down, and the peak is broad-ened and depressed. We can see from Eqs. (81) and (87) that for the same set of parameters (ζ_o, h, ω_1, V_a), the long-range, inverse-square form of ν_1/V_a^2 gives values of γ about twice as large as those obtained from the short-range exponential form. Qualitatively, of course, this could be predicted; extending collisions to higher altitudes, thereby increasing the size of the transition region without altering the

effective size of the Hall region, will increase the effect of collision broadening of the transmitted spectra.

In Figs. 2 and 3 we show $\left|T_{x,y} (\varphi = 0)\right|$ for both forms of ν_i/V_a^2. The curves for the exponential form differ from those in I because they are based on a different set of parameters. The values of γ used in I, about .3 and .45, are smaller than those derived from current ionospheric profiles.

The period τ_m of the transmission maximum is given by

$$\tau_m = \frac{2\pi}{\omega_m} = \frac{2\pi}{\omega_i} 2.5 \, \tilde{h}\tilde{\zeta}_o(1 + \gamma^2) \tag{87}$$

$$\tau_m \approx \left.\begin{array}{l} 8 \text{ seconds at sunspot minimum} \\ 22 \text{ seconds at sunspot maximum} \end{array}\right\} \frac{\tilde{\nu}_i}{\tilde{V}_a^2} = e^{z/\zeta_o}$$

$$\tau_m \approx \left.\begin{array}{l} 15 \text{ seconds at sunspot minimum} \\ 40 \text{ seconds at sunspot maximum} \end{array}\right\} \frac{\tilde{\nu}_i}{\tilde{V}_a^2} = \frac{1}{\left(1 - \frac{z}{2\zeta_o}\right)^2}$$

The numerical values of the periods given in Eq. (87) are those for high latitudes. The period would be somewhat longer at lower latitudes for the same values of $\tilde{h}$ and $\tilde{\zeta}_o$ because of the decrease in ω_i.

The maximum value of $\left|T_{x,y}\right|$ is only about 20 percent larger than its value for $\omega \to 0$ for the inverse-square form of ν_i/V_a^2. Qualitatively similar results apply to the exponential form. Thus the transmitted p-mode is slightly enhanced over a wide range of low frequencies from 0 to $2/\tau_m$. At middle-high latitudes, this corresponds to an enhancement for frequencies up to about .1 cps at sunspot minimum and up to about .04 cps at sunspot maximum; thereafter, $\left|T_{x,y}\right|$ decreases with increasing frequency.

When $\cos \varphi \neq 1$, $\left|T_x\right|$ and $\left|T_y\right|$ are equal for the exponential form of ν_i/V_a^2, and differ only slightly from each other for the inverse-square form. From Eqs. (82) and (83), we can see that the inclusion of $\cos \varphi$ effectively increases $\tilde{\zeta}$ (the increase of T_y in the inverse-

Fig. 2 -- A comparison of the magnitudes of the elemen's of the daytime magnetic transmission matrix at sunspot minimum for two forms of v_i/V_a^2, a long-range inverse square form and a short-range exponential form. The earth's field is assumed to be nearly vertical ($\cos \varphi \simeq 1$), so that $|T_x| \simeq |T_y|$.
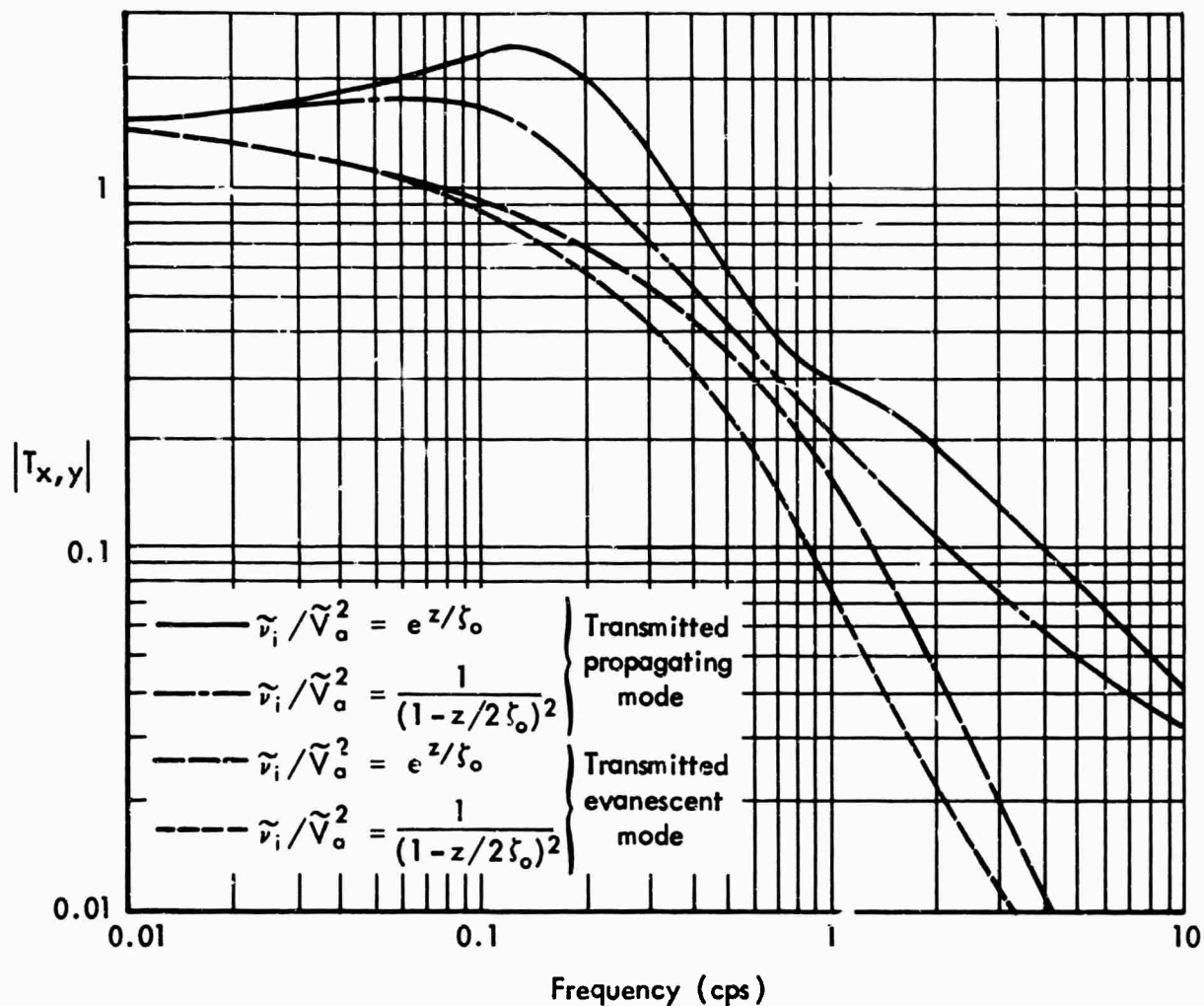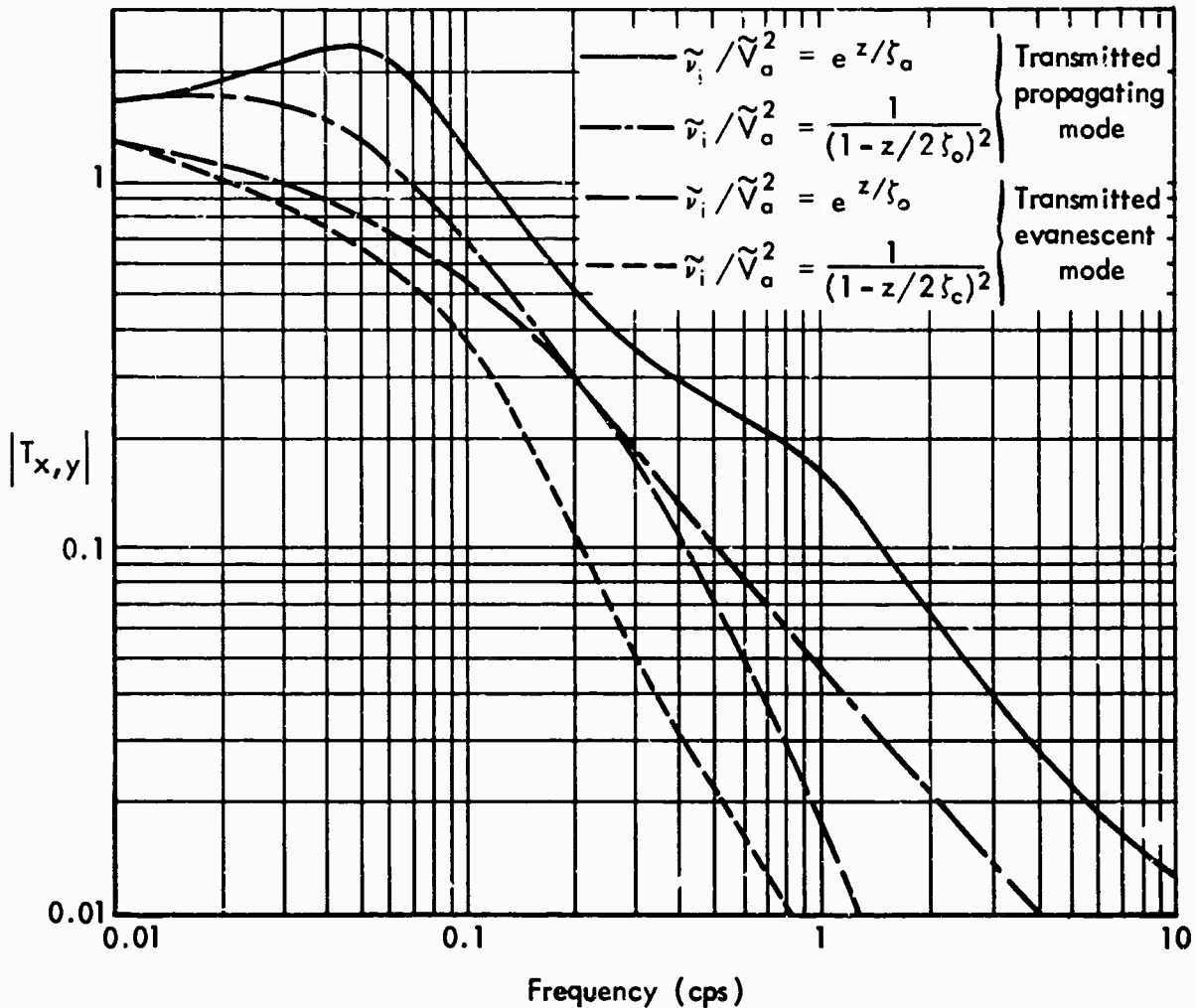
Fig. 3 -- A comparison of the magnitudes of the elements of the daytime magnetic transmission matrix at sunspot maximum for two forms of v_i/V_a^2, a long-range inverse square form and a short-range exponential form. The earth's field is assumed to be nearly vertical ($\cos \varphi \simeq 1$), so that $|T_x| \simeq |T_y|$.

square case being larger than that of T_x). Increasing $\tilde{\zeta}$ decreases the magnitude of $\left|T_{x,y}\right|$ and shifts the frequency of the maximum downwards.

So far, we have discussed only the transmitted p-mode. The transmitted e-mode can be obtained from Eqs. (80) and (81) for the exponential form of ν_i/V_a^2, and from Eqs. (80) to (84) for the inverse square form, by replacing ω by $-\omega$ and taking the complex conjugate of $T_{x,y}$. The magnitude of $T_{x,y}$ for negative ω is a monotonically decreasing function of $|\omega|$.

We shall postpone a discussion of the transmitted fields for an incident F- or S-wave for different values of φ until we have found solutions for the higher frequencies.

The approximation for small ω is valid for frequencies such that

$$\left|2.5\ \widetilde{\widetilde{\omega}}\widetilde{\zeta}_o\tilde{h}\right| < 1 \quad \text{for} \quad \frac{\tilde{\nu}_i}{\tilde{V}_a^2} = \frac{1}{\left(1 - \frac{z}{2\zeta_o}\right)^2}$$

$$\left|2\sqrt{\widetilde{\widetilde{\omega}}}\widetilde{\zeta}_o\right| < 1 \quad \text{for} \quad \frac{\tilde{\nu}_i}{\tilde{V}_a^2} = e^{z/\zeta_o}$$

At high latitudes ($\omega_i \sim 200$ rad/sec) the approximation is valid for the inverse square form of $\tilde{\nu}_i/\tilde{V}_a^2$ for frequencies less than about .25 cps at sunspot minimum and less than about .1 cps at sunspot maximum, and for the exponential form for frequencies less than about 1 cps at sunspot minimum and less than about .25 cps at sunspot maximum.

SOLUTIONS FOR HIGHER FREQUENCIES

A simple means of estimating the transmitted fields at higher frequencies is the WKB method. This approximation is applicable to an equation such as Eq. (69) when the fractional change in the magnitude of the index of refraction is small in a wavelength. The criterion for the applicability of the approximation is given in terms of q^2 by

$$\frac{1}{2} \left| \frac{dq}{d\tilde{z}} \frac{1}{q^2} \right| < 1 \tag{88}$$

In the regions in which this condition is satisfied, the solution of Eq. (69) can be approximated by a linear combination of the functions $\psi_{\pm}(\tilde{z})$, where

$$\psi_{\pm}(\tilde{z}) = \frac{e^{\pm i \int^{\tilde{z}} q d\tilde{z}}}{\sqrt{q}} \tag{89}$$

For the function q^2 given by Eqs. (64) and (65), Eq. (88) is satisfied if

$$|4\sqrt{\tilde{\omega}}\tilde{\zeta}_o| > 1 \quad \text{for} \quad \frac{\tilde{\nu}_1}{\tilde{v}_a^2} = \frac{1}{\left(1 - \frac{z}{2\zeta_o}\right)^2}$$

$$|8 \tilde{\omega}\tilde{\zeta}_o| > 1 \quad \text{for} \quad \frac{\tilde{\nu}_1}{\tilde{v}_a^2} = e^{z/\zeta_o}$$

These conditions essentially cover the frequency range in which the low-frequency approximation breaks down.

The application of the WKB method to   solution of Eq. (69) involves some subtleties (especially in the case of negative frequencies), which are discussed in the Appendix. In this section we present the results.

For positive frequencies (denoted by the subscript p, since they correspond to the propagating mode), the approximate solution of Eq. (69) is given by

$$\mathcal{E}_p(u) \approx \frac{2i}{c}\left[E_x - iB_y \cos \varphi\right]_{inc} \exp\left[i\int_{u_o}^{u_1} q_p(u)du\right]$$

$$\times \left[\frac{q_p(u_o)}{q_p(u)}\right]^{1/2}\left[\cos \int_u^{u_1} q_p(u)du\right] \tag{90}$$

where

$$u = -\log\left(e^{-\pi/2}\frac{\tilde{\nu}_i}{\tilde{\gamma}_a^2}\right) = -\frac{z}{\zeta_o} - \frac{i\pi}{2} \tag{91}$$

$$q_p^2(u) = \tilde{\omega}^2\tilde{\zeta}_o^2\left[\frac{e^u + \frac{1}{\tilde{\omega}}}{a_{x,y}e^u + \cos \varphi}\right] \tag{92}$$

$$\left.\right\} \quad \frac{\tilde{\nu}_i}{\tilde{\gamma}_a^2} = e^{z/\zeta_o}$$

$$u = \left[e^{i\pi/2}\frac{\tilde{\nu}_i}{\tilde{\gamma}_a^2}\right]^{-1/2} = \left(1 - \frac{z}{2\zeta_o}\right)e^{-\frac{i\pi}{4}} \tag{93}$$

$$q_p^2(u) = 4\tilde{\omega}^2\tilde{\zeta}_o^2\, e^{i\pi/2}\left[\frac{u^2 + \frac{1}{\tilde{\omega}}}{a_{x,y}u^2 + \cos \varphi}\right] \tag{94}$$

$$\left.\right\} \quad \frac{\tilde{\nu}_i}{\tilde{\gamma}_a^2} = \frac{1}{\left(1 - \frac{z}{2\zeta_o}\right)^2}$$

$$u_o \equiv u(\tilde{z}_o) \tag{95}$$

$$u_1 \equiv u(\tilde{z}_1) \tag{96}$$

$$a_x = 1 \tag{97}$$

$$a_y = \cos^2 \varphi \tag{98}$$

As before, the choice of the subscript x or y depends upon the boundary conditions on the incident wave.

At the bottom of the ionosphere ($\tilde{z} = \tilde{z}_1$), Eq. (90) becomes

$$
\mathcal{E}_p(\tilde{z}_1) = \frac{2i}{c}\left[B_x - iB_y \cos \varphi\right]_{inc}\left(\frac{\cos \varphi}{a_{x,y}}\right)^{1/2} \tilde{\omega}^{1/4} \exp i\int_{u_o}^{u_1} q_p(u)\,du
$$

(99)

From Eq. (99) we obtain the magnitude of the positive-frequency elements of the transmission matrix:

$$
\left|T_x(\varphi)\right|_p = \frac{\sqrt{2}}{\tilde{\omega}^{3/4}\,\tilde{h}} (\cos \varphi)^{1/4} \exp\left[- \text{Im} \int_{u_o}^{u_1} q_{px}(u)\,du\right]
$$

(100)

$$
\left|T_y(\varphi)\right|_p = \frac{\sqrt{2}}{\tilde{\omega}^{3/4}\,\tilde{h}} (\cos \varphi)^{3/4} \exp\left[- \text{Im} \int_{u_o}^{u_1} q_{py}(u)\,du\right]
$$

(101)

where $\text{Im} \int q\,du$ denotes the imaginary part of the integral.

The effects of collisional absorption are contained in the exponential terms in Eqs. (100) and (101). The factor $\tilde{\omega}^{1/4}$ in $\mathcal{E}(\tilde{z}_1)$ (which leads to the factor $\tilde{\omega}^{-3/4}$ in $\mathcal{B}_{Ground}$ and in $|T_{x,y}|$) is a consequence of the increase in the index of refraction (for $\tilde{\omega} < 1$) by a factor of $\tilde{\omega}^{-1/2}$ between the Alfvén and Hall regions. The amplitude of the electric field in each region is inversely proportional to the square root of the region's index of refraction.

Evaluating the integrals in Eqs. (100) and (101) for both the exponential and inverse square forms of ν_i/V_a^2, we obtain

$$\left|T_x(\varphi)\right|_p = \frac{\sqrt{2}}{\tilde{\omega}^{3/4}\,\tilde{h}}\,(\cos\varphi)^{1/4}\,e^{-\frac{\pi}{2}\tilde{\zeta}_o\sqrt{\frac{\tilde{\omega}}{\cos\varphi}}\,(1-\sqrt{\tilde{\omega}\cos\varphi})} \tag{102}$$

$$\left|T_y(\varphi)\right|_p = \frac{\sqrt{2}}{\tilde{\omega}^{3/4}\,\tilde{h}}\,(\cos\varphi)^{3/4}\,e^{-\frac{\pi}{2}\sqrt{\frac{\tilde{\omega}}{\cos\varphi}}\,\tilde{\zeta}_o\left(1-\sqrt{\frac{\tilde{\omega}}{\cos\varphi}}\right)} \tag{103}$$

$$\left.\right\}\quad \frac{\tilde{\nu}_1}{\tilde{V}_a^2} = e^{z/\zeta_o}$$

$$\left|T_x(\varphi)\right|_p \approx \frac{\sqrt{2}}{\tilde{\omega}^{3/4}\,\tilde{h}}\,(\cos\varphi)^{1/4}\,e^{-\sqrt{2\tilde{\omega}}\,\tilde{\zeta}_o\,\ln\frac{1}{\sqrt{\tilde{\omega}}}} \tag{104}$$

$$\left|T_y(\varphi)\right|_p \approx \frac{\sqrt{2}}{\tilde{\omega}^{3/4}\,\tilde{h}}\,(\cos\varphi)^{3/4}\,e^{-\sqrt{2\tilde{\omega}}\,\frac{\tilde{\zeta}_o}{\cos\varphi}\,\ln\frac{1}{\sqrt{\tilde{\omega}}}} \tag{105}$$

$$\left.\right\}\quad \frac{\tilde{\nu}_1}{\tilde{V}_a^2} = \frac{1}{\left(1-\frac{z}{2\zeta_o}\right)^2}$$

To compare the results for the two forms of ν_1/V_a^2, we let $\cos\varphi \sim 1$ and use a value of $\omega_1 \approx 200$ rad/sec appropriate to high latitudes.

We then obtain

$$\left|T_{x,y}(0)\right|_p^{\substack{\text{sunspot}\\\text{min}}} \approx \frac{.7}{f^{3/4}}\,e^{-.7\sqrt{f}(1-.17\sqrt{f})} \tag{106}$$

$$\left|T_{x,y}(0)\right|_p^{\substack{\text{sunspot}\\\text{max}}} \approx \frac{.5}{f^{3/4}}\,e^{-1.4\sqrt{f}(1-.17\sqrt{f})} \tag{107}$$

$$\left.\right\}\quad \frac{\tilde{\nu}_1}{\tilde{V}_a^2} = e^{z/\zeta_o}$$

$$\left|T_{x,y}(0)\right|_p^{\substack{\text{sunspot}\\\text{min}}} \approx \frac{.7}{f^{3/4}}\,e^{-1.2\sqrt{f}(1+\frac{3}{5}\ln\frac{1}{\sqrt{f}})} \tag{108}$$

$$\left|T_{x,y}(0)\right|_p^{\substack{\text{sunspot}\\\text{max}}} \approx \frac{.5}{f^{3/4}}\,e^{-2.4\sqrt{f}(1+\frac{3}{5}\ln\frac{1}{\sqrt{f}})} \tag{109}$$

$$\left.\right\}\quad \frac{\tilde{\nu}_1}{\tilde{V}_a^2} = \frac{1}{\left(1-\frac{z}{2\zeta_o}\right)^2}$$

where f is the frequency in cps.

For both forms of ν_i/V_a^2, the major frequency-dependence of $|T|_p$ is provided by the factor $1/f^{3/4}$. This is due to the fact that the exponential term in $|T|_p$ does not vary much in this frequency range, indicating that the collisional attenuation apparently does not depend much upon frequency.

Although the exponential term in the elements of the transmission matrix does not vary much with frequency for either the exponential or inverse-square form of ν_i/V_a^2, its value is different in the two cases, the attenuation being predictably larger for the long-range than for the short-range form. The fractional difference between the elements of the transmission matrix for the exponential and inverse-square forms is appreciable (especially at sunspot maximum) at frequencies below a few cps, but becomes smaller as the frequency approaches the ion cyclotron-frequency. This is a consequence of the "shrinking" of the transition region as the frequency increases.

When $\cos \varphi \neq 1$, we can see from Eqs. (102) to (105) that $|T_y|_p < |T_x|_p$. The ratio of $|T_y|_p$ to $|T_x|_p$ is smaller for the inverse-square form than for the exponential form, and for the inverse-square form is

$$\frac{|T_y|_p}{|T_x|_p} \approx (\cos \varphi)^{1/2}\left[1 - 1.2\sqrt{f}\left(1 + \frac{3}{5}\ln\frac{1}{\sqrt{f}}\right)(\sec \varphi - 1)\right] \qquad (110)$$

at sunspot minimum, and

$$\frac{|T_y|_p}{|T_x|_p} \approx (\cos \varphi)^{1/2}\left[1 - 2.4\sqrt{f}\left(1 + \frac{3}{5}\ln\frac{1}{\sqrt{f}}\right)(\sec \varphi - 1)\right] \qquad (111)$$

at sunspot maximum.

When $\varphi \sim 30$ deg and $f \sim 1$ cps, the ratio is about 0.7 at sunspot minimum and about 0.5 at sunspot maximum, and decreases as φ increases.

For negative frequencies (denoted by the subscript e, since they correspond to the evanescent mode), the approximate solution of Eq. (69) is given by

$$\ell_e(v) \approx - \frac{2i}{c} (B_x - iB_y \cos \varphi)_{inc} \exp\left[i\left(\int_{v_2}^{v_o} |\frac{q_e(v)}{q_e(v_o)}| q_e(v_o)dv - \frac{\pi}{4}\right)\right]$$

$$\times \cos\left[\int_{v_2}^{v} |\frac{q_e(v)}{q_e(v_o)}| q_e(v_o)dv - \frac{\pi}{4}\right] \quad \text{for} \quad v \gg v_2 \quad (112)$$

$$\ell_e(v) \approx \frac{2i}{c} (B_x - iB_y \cos \varphi)_{inc}\tilde{\omega}^{1/4}\left[v^2 + \frac{\cos \varphi}{a_{x,\cdot}}\right]^{1/4}$$

$$\times \exp\left[i\left(\int_{v_2}^{v_o} |\frac{q_e(v)}{q_e(v_o)}| q_e(v_o)dv - q_e(v_o) \int_{v}^{v_2} |\frac{q_e(v)}{q_e(v_o)}| dv\right)\right] \quad (113)$$

$$\text{for } v \ll v_2$$

where

$$v \equiv u^* \quad (114)$$

$$\ell_e(v) \equiv \ell^*(-\omega, u^*) \quad (115)$$

$$q_e(v) \equiv q^*(-\omega, u^*) \quad (116)$$

and v_2 is defined by

$$q_e(v_2) = 0 \quad (117)$$

From $\ell_e(v_1)$ we can find $[B^*(-\omega)]_{Ground}$ and the negative-frequency elements of the transmission matrix. The results are given by

$$|T_x(\varphi)|_\rho \simeq e^{-\sqrt{|\tilde{\omega}|}\ \tilde{z}_1}\ |T_x(\varphi)|_p \tag{118}$$

$$\frac{\tilde{\nu}_1}{V_a^2} = e^{z/\zeta_o}$$

$$|T_y(\varphi)|_e \simeq e^{-\sqrt{\frac{|\tilde{\omega}|}{\cos\varphi}}\ \tilde{z}_1}\ |T_y(\varphi)|_p \tag{119}$$

$$|T_x(\varphi)|_e \simeq e^{-\frac{\pi}{2}\sqrt{2}\sqrt{|\tilde{\omega}|}\ \zeta_o}\ |T_x|_p \tag{120}$$

$$\frac{\tilde{\nu}_1}{V_a^2} = \frac{1}{\left(1 - \frac{z}{2\zeta_o}\right)^2}$$

$$|T_y(\varphi)|_e \simeq e^{-\frac{\pi}{2}\sqrt{2}\sqrt{|\tilde{\omega}|}\ \frac{\zeta_o}{\cos\varphi}}\ |T_y|_p \tag{121}$$

The transmitted amplitude of the e-mode falls off exponentially with $\sqrt{|\tilde{\omega}|}$ for $|\omega|$ larger than about 4 rad/sec at sunspot minimum and for $|\omega|$ larger than about 1 rad/sec at sunspot maximum. This applies to both forms of ν_i/V_a^2, although the magnitudes of the transmitted amplitudes differ for the two cases because of differing amounts of collisional absorption. The exponential decrease of amplitude with $\sqrt{|\omega|}$ is a consequence of the evanescence in the Hall region, and is not the result of true absorption. In Figs. 2 and 3 we show $|T_{x,y}|_{p,e}$ when $\cos\varphi \simeq 1$ for both forms of ν_i/V_a^2.

Our analytical approximations (using the inverse-square form of ν_i/V_a^2) are compared with the numerical results of III in Figs. 4 and 5. They agree well for $|T_x|_p$ at frequencies up to about 5 cps and for $|T_y|_p$ at frequencies up to about 1 cps. Our approximations give larger values for $|T_{x,y}|_e$ than those of III, the error becoming fairly large at the higher frequencies; this is not surprising, in view of

Fig. 4 -- A comparison between the analytic approximations to the
elements of the daytime magnetic transmission matrix obtained
in this paper (using the inverse square form of v_i/V_a^2) and
the numerical values obtained by Karplus, Francis, and
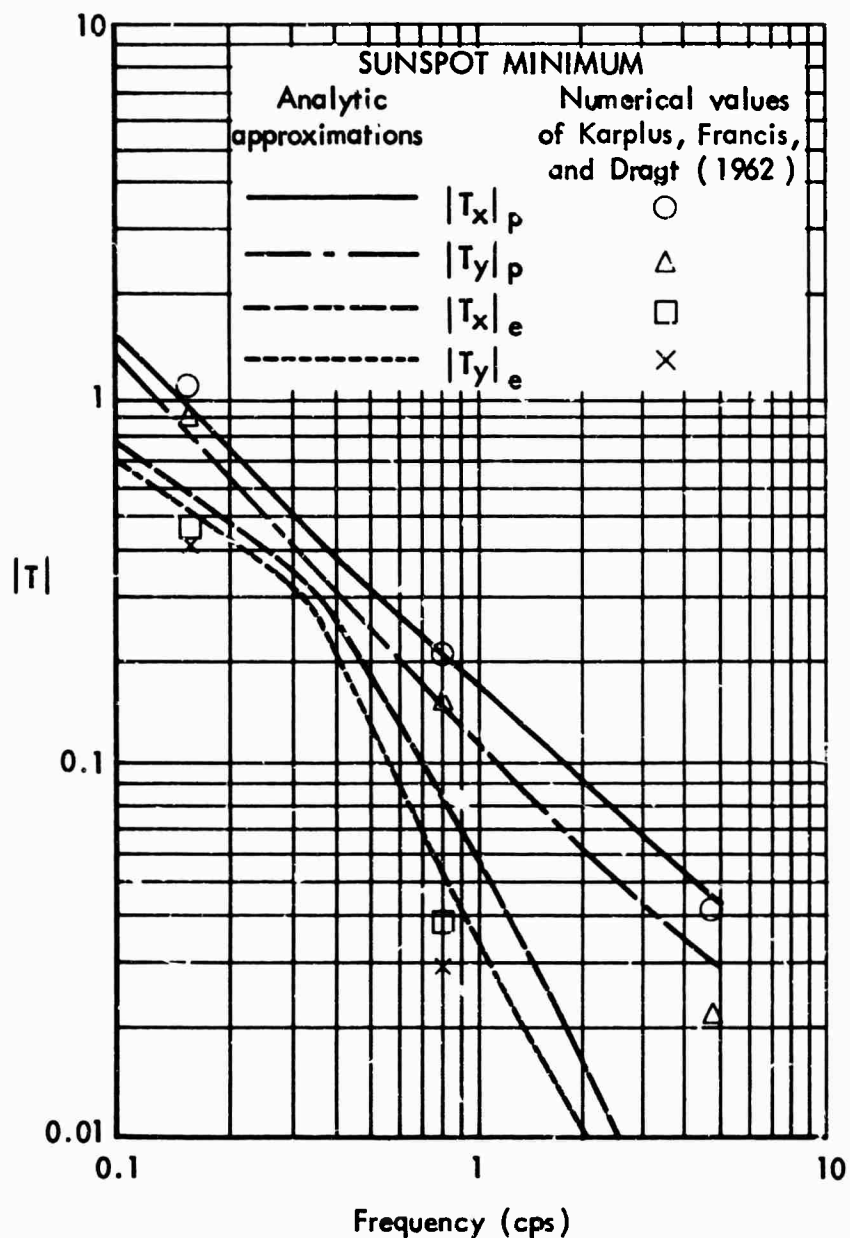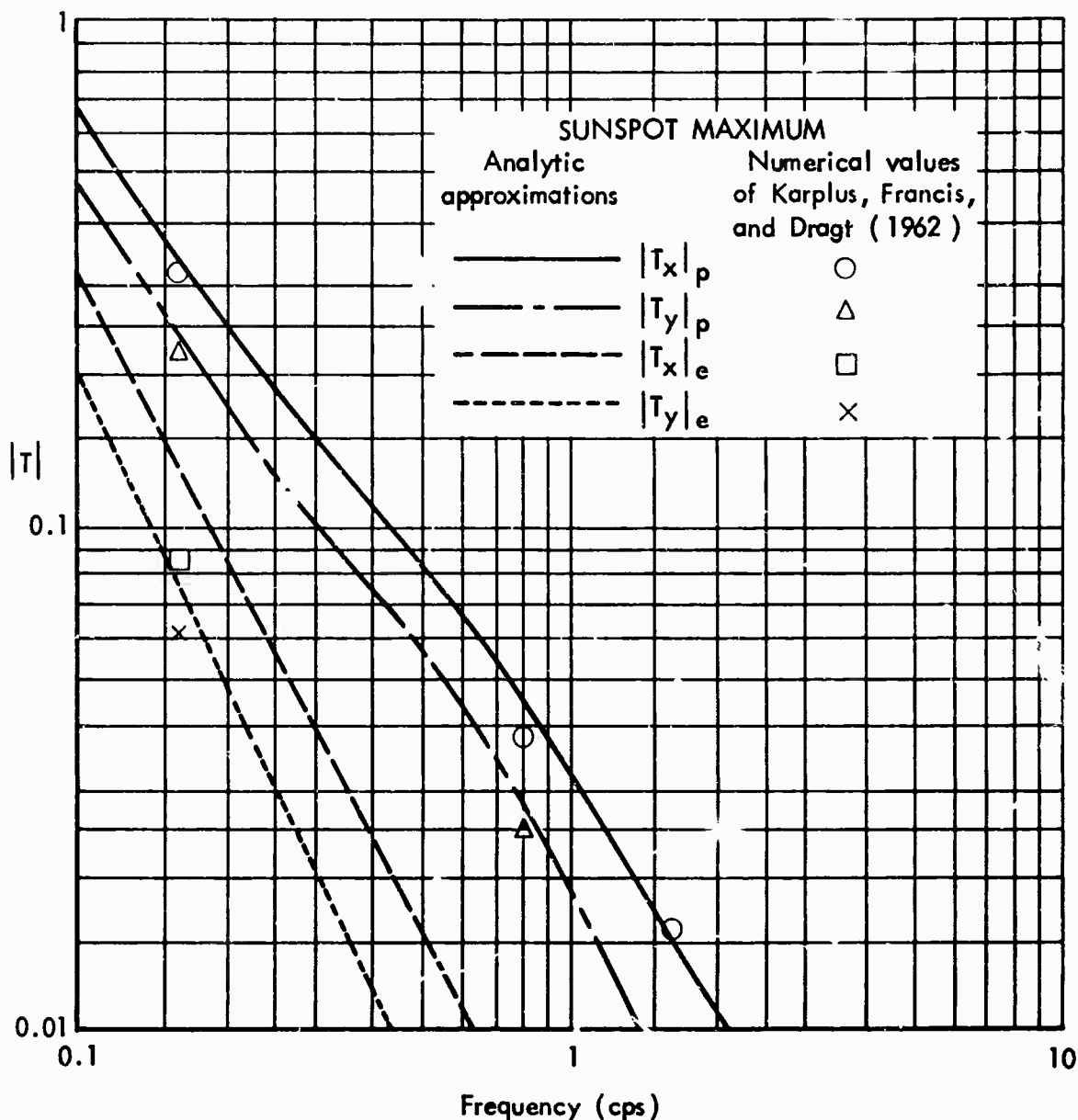Dragt (1962). The magnetic dip angle is assumed to
be 60°.

Fig. 5 -- A comparison between the analytic approximations to the elements of the daytime magnetic transmission matrix obtained in this paper (using the inverse-square form of v_i/V_a^2) and the numerical values obtained by Karplus, Francis, and Dragt (1962). The magnetic dip angle is assumed to be 60°.

the exponential nature of the frequency-dependence of $|T|_e$. However, except under certain conditions, which we shall discuss shortly, the transmitted field consists almost entirely of the p-mode at frequencies above about .5 cps, and we need not be concerned with the small amount of e-mode that is transmitted.

Having found the transmission matrix elements, we can now find $|B|_{Ground}$ for an incident F- or S-wave from Eqs. (48) to (57):

Incident F-Wave

$$|B|_{Ground} = \left[|T_x(\varphi)|_p^2 + |T_x(\varphi)|_e^2 \right]^{1/2} \qquad \varphi > \sqrt{2\tilde{\omega}} \qquad (122)$$

$$|B|_{Ground} = \left[\frac{4\left(1 - \frac{\varphi^2}{4\tilde{\omega}}\right)^2 |T(0)|_p^2 + \left(\frac{\varphi^2}{2\tilde{\omega}}\right)^2 |T(0)|_e^2}{\left(1 - \frac{\varphi^2}{2\tilde{\omega}}\right)^2 + 1} \right]^{1/2} \qquad \varphi < \sqrt{2\tilde{\omega}} \qquad (123)$$

$$|B|_{Ground} \rightarrow \sqrt{2}\, |T(0)|_p \quad \text{as } \varphi \rightarrow 0 \qquad (124)$$

Incident S-Wave

$$|B|_{Ground} = \left[|T_y(\varphi)|_p^2 + |T_y(\varphi)|_e^2 \right]^{1/2} \qquad \varphi > \sqrt{2\tilde{\omega}} \qquad (125)$$

$$|B|_{Ground} = \left[\frac{4\left(1 - \frac{\varphi^2}{4\tilde{\omega}}\right)^2 |T(0)|_e^2 + \left(\frac{\varphi^2}{2\tilde{\omega}}\right)^2 |T(0)|_p^2}{\left(1 - \frac{\varphi^2}{2\tilde{\omega}}\right)^2 + 1} \right]^{1/2} \qquad \varphi < \sqrt{2\tilde{\omega}} \qquad (126)$$

$$|B|_{Ground} \rightarrow \sqrt{2}\, |T(0)|_e \quad \text{as } \varphi \rightarrow 0 \qquad (127)$$

In Fig. 6, we show $|B|_{Ground}$ as a function of φ for incident S- and F-waves of frequencies .5, 1, and 2 cps for minimum sunspot conditions. For $T_{x,y}(\varphi)$ in Eqs. (122) to (127) we have used the values obtained with the inverse square form of v_i/V_a^2.

PAGES 45-46

ARE

MISSING

IN

ORIGINAL

DOCUMENT

VII. DEPENDENCE OF DAYTIME TRANSMISSION CHARACTERISTICS
ON IONOSPHERIC ELECTRON DENSITY

So far, we have expressed the elements of the transmission matrix in terms of dimensionless variables whose units of frequency and length are given by:

$$\omega_{1o} \text{ (unit of frequency)} \simeq 210 \cos \varphi \text{ rad/sec (at nonequatorial latitudes)}$$

$$\tag{128}$$

$$\frac{V_{ao}}{\omega_{1o}} \text{ (unit of length)} = \frac{1.2}{(\bar{N}_{1o})^{1/2}} \text{ km} \tag{129}$$

where

$$\bar{N}_{1o} = N_{1o} \text{ in (No./cc)} \times 10^{-6} \tag{130}$$

and the subscript o refers to $z = 0$ (the altitude at which $\nu_1 = \omega_1$). The order of magnitude of $\bar{N}_{1o}$ is .1 under normal daytime conditions. (In our calculations we have used values of $\bar{N}_{1o}$ of .1 at sunspot minimum and .175 at sunspot maximum.)

Let us examine the dependence of the daytime transmission characteristics on $\bar{N}_{1o}$. First, we express the quantity $4\sqrt{|\tilde{\omega}|}\tilde{\zeta}_o$ in terms of N_{1o}, since this quantity determines which of the approximate solutions of the propagation equations is applicable. The quantity $4\sqrt{|\tilde{\omega}|}\tilde{\zeta}_o$ is given by

$$4\sqrt{|\tilde{\omega}|}\tilde{\zeta}_o \approx \frac{7}{12} \sqrt{\frac{f}{\cos \varphi}} \zeta_o (\bar{N}_{1o})^{1/2} \tag{131}$$

where ζ_o is in km. According to the profiles of Sims and Bostick, ζ_o appears to increase with $\bar{N}_{1o}$. Using the numerical values for minimum and maximum sunspot conditions, we can obtain an approximate empirical relationship between ζ_o and $\bar{N}_{1o}$:

$$\frac{\zeta_o}{10} \approx (10 \ \overline{N}_{1o})^{3/4} \tag{132}$$

which gives

$$4\sqrt{|\widetilde{\omega}|}\widetilde{\zeta}_o \approx 2 \sqrt{\frac{f}{\cos \varphi}} (10 \ \overline{N}_{1o})^{5/4} \tag{133}$$

When $2\sqrt{f}(10 \ \overline{N}_{1o})^{5/4} < 1$, we use the results of the low-frequency approximation. We have seen that at these low frequencies, γ and $\widetilde{\zeta}_o/\widetilde{\omega}_1$ are the quantities determining the transmission characteristics, particularly the period, the height, and the width of the p-mode transmission maximum. Since γ is the dimensionless ratio of the effective size of the transition region to the size of the Hall region, its value is independent of the unit of length.

For τ_m, the period at the transmission maximum, we have obtained [Eq. (87)] from the low-frequency approximation

$$\tau_m \approx \frac{2\pi\widetilde{\widetilde{\zeta}}_o \ 2.5(1 + \gamma^2)}{\omega_1}$$

$$\approx \frac{2\pi\zeta_o}{\cos \varphi} (1 + \gamma^2)\overline{N}_{1o} \text{ seconds} \tag{134}$$

Since the transmitted p-mode is enhanced for frequencies up to about $2/\tau_m$, larger particle densities result in a smaller range of frequencies of enhanced transmission.

When $2\sqrt{f}(10 \ \overline{N}_{1o})^{5/4} > 1$, the positive frequency transmission matrix elements are given by

$$|T_{x,y}|_p \cong \frac{.7}{(10 \ \overline{N}_{1o})^{1/2}} \frac{1}{f^{3/4}} \times$$

$$\exp\left[- 1.2 \sqrt{\frac{f}{a_{x,y} \cos \varphi}} \frac{\zeta_o}{10} (10 \ \overline{N}_{1o})^{1/2}\left(1 + \frac{3}{5} \ \ell n \ \sqrt{\frac{\cos \varphi}{f}}\right)\right] \tag{135}$$

The exponent in Eq. (135) is based on the inverse-square form of ν_i/V_a^2, which seems to give a reasonably good fit to current ionospheric profiles. Since the exponent in Eq. (135) is of the order of unity for f near 1, small variations of $10\,\overline{N}_{1o}$ about unity will not have much effect on $|T|_p$.

The transmitted e-mode is more critically affected by changes in $\overline{N}_{1o}$. For $|T_{x,y}|_e$, we have

$$|T_{x,y}|_e \approx \exp\left[-1.1\,\sqrt{\frac{f}{\cos\varphi}}\,\frac{\zeta_o}{10}\,(10\,\overline{N}_{1o})^{1/2}|T_{x,y}|_p\right]$$

$$\approx \frac{f^{3/4}}{.7}\,(10\,\overline{N}_{1o})^{1/2}|T_{x,y}|_p^2 \quad \text{for f near 1.} \tag{136}$$

Thus the attenuation of the e-mode increases roughly as the square of the attenuation of the p-mode as $\overline{N}_{1o}$ increases. When $\varphi > \sqrt{2\tilde{\omega}}$ (or for dip angles less than about 75° for $f \sim 1$ cps), the e-mode does not contribute much to the transmitted fields and we need not be concerned with $|T|_e$. For the daylight polar regions, appreciable increases in N_{1o} would result in a sizeable reduction in the transmitted amplitude of an incident S-wave, since such a wave gives rise mainly to a transmitted e-mode.

In Fig. 7, we show $|B|_{Ground}$ for s .spot minimum and maximum daytime conditions for $f = .25, .5, 1,$ and 2 cps, and for a dip angle of 74°. From Fig. 7, we can see that the equation

$$|B|_{Ground} = 1.3\,\frac{e^{-1.85(10\,\overline{N}_{1o})}}{f} \tag{137}$$

gives a good fit to the theoretically calculated points. We can use Eq. (137) to estimate $|B|_{Ground}$ at middle latitudes for frequencies in the range $1/4 \le f \le 2$ cps and for values of $\overline{N}_{1o}$ not much less than 0.1 (sunspot minimum) or much greater than .175 (sunspot maximum). (Extrapolation to values of $\overline{N}_{1o}$ much outside the range shown in Fig. 7

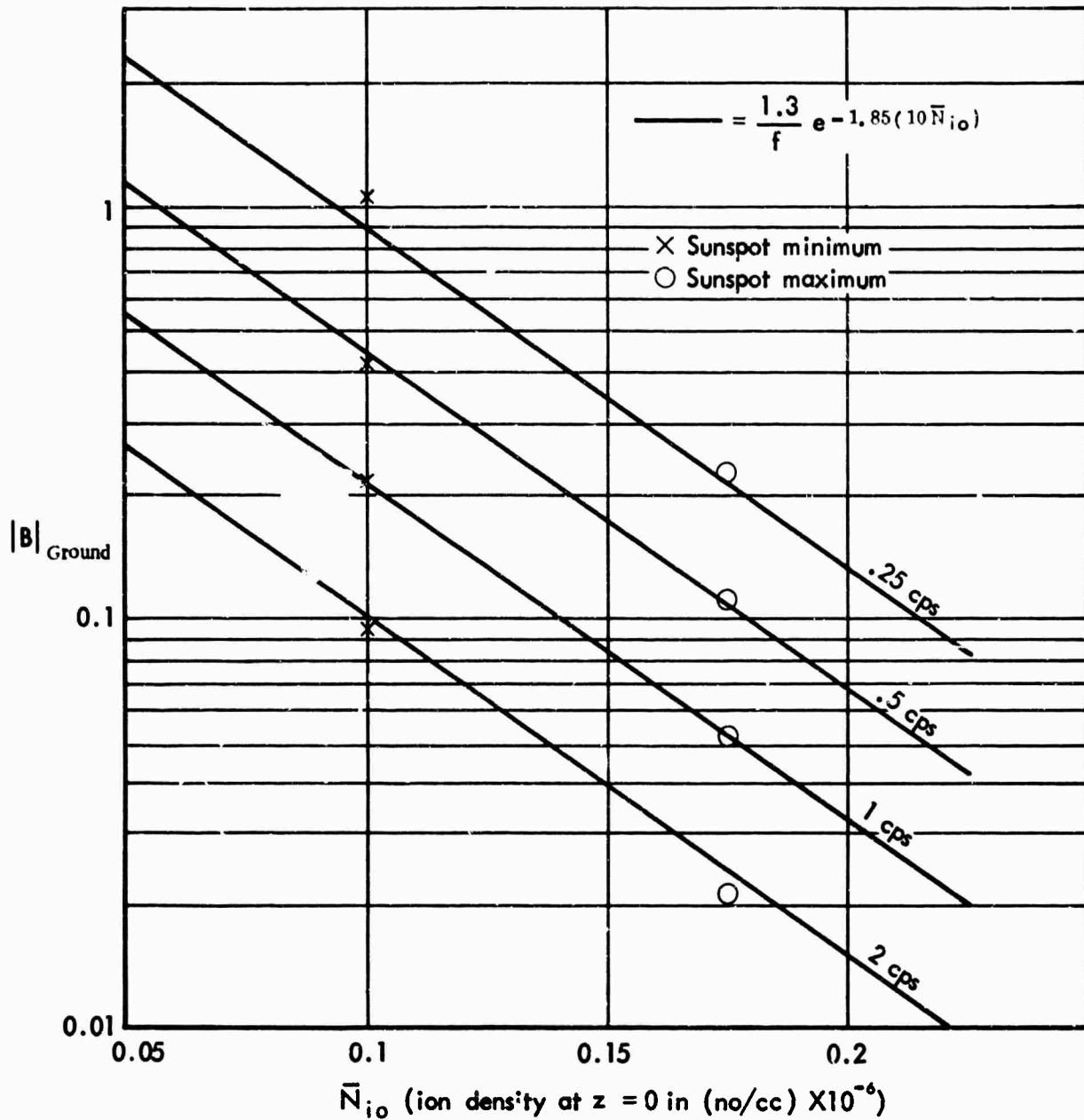Fig 7 -- The amplitude of the daytime ground-level magnetic signal as a function of the ion density at z = 0. The data points are obtained from the analytic approximations to $|B|_{Ground}$ derived in the text; the numerical values of the parameters are from Sims and Bostick (1963) for minimum and maximum sunspot conditions and a magnetic dip angle of 74°. The solid curves are empirical fits to the data points given by Eq. (137).

cannot be justified without more information on the variation of ζ_o with $\overline{N}_{io}$.)

From Eq. (137) we see that for a given frequency in the frequency range of .25 to 2 cps, an increase in electron density of the lower ionosphere of about 55 percent results in a reduction of the transmitted amplitude of about $1/e$. The shape of the amplitude-frequency curve is insensitive to $\overline{N}_{io}$ because of the insensitivity of the collisional attenuation to frequency. This implies that variations in daytime electron density (with season, time of day, and solar activity) should not materially affect the relative transmitted amplitudes for different frequencies between about .25 and 2 cps, unless the relative amplitudes of the incident fields in the lower Alfvén region are affected.

Let us compare Eq. (137) with an empirical equation obtained by Wentworth (1964) from the numerical results of III. Wentworth related the attenuation $1/|B|_{Ground}$ to the frequency and to the F_2 ion-density maximum by the equation

$$\text{attenuation} \equiv \frac{1}{|B|_{Ground}} = 1 + \frac{f(f_oF_2)^4}{400} \tag{138}$$

where f_oF_2 is the plasma frequency at the F_2 ion-density maximum in megacycles/sec, and is given by

$$1.24 \times 10^4 \frac{(f_oF_2)^2}{cm^3} = \text{ion density at } F_2 \text{ peak} \tag{139}$$

When $f > .25$ cps and F_2 peak ion densities are greater than about $.5 \times 10^6$ per cm^3, Eq. (138) becomes

$$|B|_{Ground} \approx \frac{400}{f(f_oF_2)^4} \tag{140}$$

The frequency dependence of Eq. (140) agrees with Eq. (137). A further comparison between Eqs. (137) and (140) is difficult, since Eq. (140) relates $|B|_{Ground}$ directly to the F_2 peak ion density, whereas Eq. (137) relates $|B|_{Ground}$ to the ion density in the lower ionosphere. Since the lower ionosphere is the region in which most of the collisional attenuation occurs, it seems preferable to us to relate the attenuation directly to ion densities in this region, rather than to those at the F_2 maximum, even though more information is usually available concerning the latter.

Our theoretical results are supported by recently reported experimental observations. Dawson (1967) reports no particular correlation between amplitudes (of disturbances in the pc 1 frequency range) and ionospheric parameters at College, Alaska (65°N), in agreement with our prediction that moderate fluctuations in N_{io} have little effect on $|B|_{Ground}$. From observations of hydromagnetic emissions of frequencies .5, .75, and 1 cps made at Baie St. Paul, Quebec (47°N), Campbell (1967) reports a decrease in daytime amplitudes by a factor between 1.5 and 3 as the Kp index increases from 0 to 3+. The relative amplitudes at the different frequencies vary little, however, with the Kp index. Furthermore, there is no discernible dependence of the daytime amplitude ratios on the solar zenith angle.

So far we have considered only daytime transmission. In the next section we shall consider the day--night ratio of transmitted amplitudes.

VIII. DAY-NIGHT AMPLITUDE RATIOS

For waves of frequencies below a few cps, the "bottom" of the nighttime ionosphere is located in the Alfvén region, at an altitude of about 300 km. At lower altitudes, the Alfvén speed is sufficiently large that the medium behaves essentially like a vacuum.

Within the nighttime ionosphere, the fields have the form of Eqs. (37) to (40). If the origin of the coordinate system is taken at the base of the ionosphere, the boundary condition on E at $z = 0$ is given by

$$\left(\frac{dE_{x,y}}{dz}\right)_{z=0} = -\frac{1}{\tilde{H}} E_{x,y}(z = 0) \tag{141}$$

where H is the height of the nighttime earth--ionosphere cavity. We can then obtain $E_{x,y}(z = 0)$ in terms of A_x and A_y:

$$E_x(z = 0) = A_y \frac{\cos \varphi}{\tilde{c}} \left[\frac{2i\tilde{k}_y \tilde{H}}{i\tilde{k}_y \tilde{H} - 1}\right] \tag{142}$$

$$E_y(z = 0) = -\frac{A_x}{\tilde{c}} \left[\frac{2i\tilde{k}_x \tilde{H}}{i\tilde{k}_x \tilde{H} - 1}\right] \tag{143}$$

Applying the induction equation at the surface of the earth, and using the boundary conditions [Eqs. (48) to (52)] to give A_x and A_y, we get for $|B|_{Ground}$

$$|B|_{Ground}^{night} = \frac{2}{\sqrt{1 + \tilde{k}_{x,y}^2 \tilde{H}^2}} \tag{144}$$

If we use the parameters appropriate to high latitudes obtained from Sims and Bostick, Eq. (144) becomes

$$|B|_{Ground} \approx \frac{1}{f} \left[10 \, \bar{N}_{io}\right]^{-1/2} \left[1 + \frac{1}{4f^2(10 \, \bar{N}_{io})}\right]^{-1/2} \qquad (145)$$

The approximate day--night amplitude ratio when $1/4 < f \lesssim 2$ cps, $0.5 \lesssim \bar{N}_{io} \lesssim .22$, and $\varphi > \sqrt{2\bar{\omega}}$ is given by[*]

$$\frac{|B|_{Ground}^{Day}}{|B|_{Ground}^{Night}} \approx 1.3 \, \exp\left[-1.85(10 \, \bar{N}_{io})\right] \left[10 \, \bar{N}_{io}\right]^{1/2} \left[1 + \frac{1}{4f^2(10 \, \bar{N}_{io})}\right]^{1,2}$$

$$(146)$$

(We have let $\cos \varphi = 1$, since $\cos \varphi$ varies only slightly for values of φ appropriate to middle and high latitudes, and the dependence on φ is furthermore obscured by the uncertainty in the value of H.) Let us note that daytime collisional absorption is not the only factor influencing this ratio; the ratio of the heights of the effective nighttime and daytime earth--ionosphere cavities also plays an important role. We can see from Eq. (146) that for frequencies larger than about $1/2(10 \, \bar{N}_{io})^{1/2}$, the day--night amplitude ratio becomes almost independent of frequency. Figure 3 shows the day--night amplitude ratio for frequencies in the range $.25 \leq f \leq 2$ cps for values of $\bar{N}_{io}$ of .05, .1, .15, and .2.

These results can be compared with the experimental observations reported by Campbell (1967) on the relative signal amplitudes of hydromagnetic emissions received at magnetically conjugate stations during periods of changing ionospheric illumination. The stations studied are at Eights, Antarctica (75°S, 77°W) and Baie St. Paul, Quebec (47°N, 70°W). Events occurring simultaneously at the two sites were recorded, with a preferred selection of events which occurred when the Antarctic station remained in darkness as its Canadian conjugate progressed through day--night cycles. The day-night amplitude ratios obtained ranged from .2 to .7, depending upon the Kp index for low Kp indices between 0 and 3+, and for frequencies between .5 and 1 cps. These

---

[*]In Eqs. (145) and (146), $\bar{N}_{io}$ refers to its daytime value.
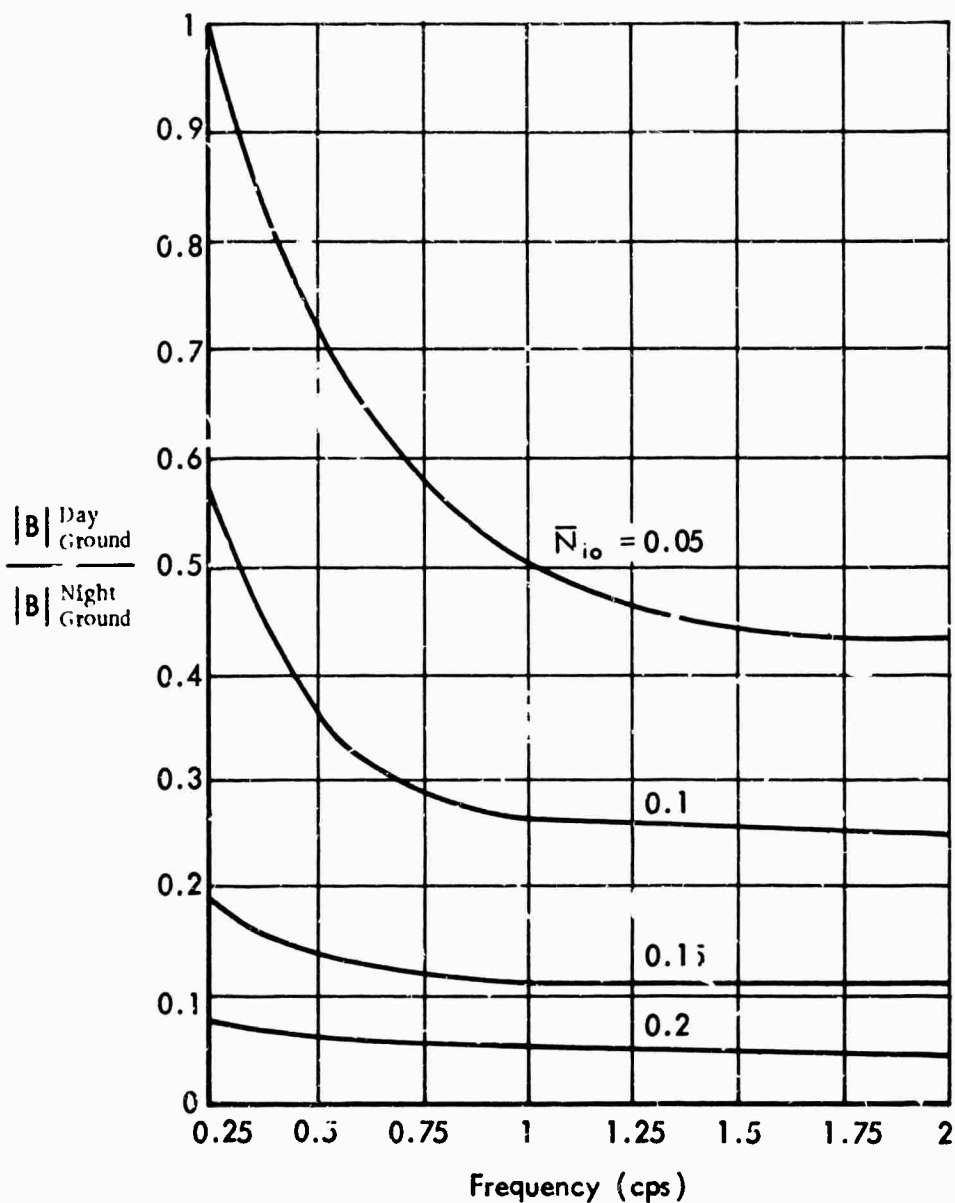
Fig. 8 -- The ratio of the amplitude of the daytime
to the amplitude of the nighttime ground-level
magnetic signal for a given incident
field amplitude as a function of
frequency and daytime ion
density at $z = 0$.

results are entirely consistent with our theoretical results for
$.5 \lesssim 10 \, \overline{N}_{1o} \lesssim 1.5$, especially considering the uncertainty of the parameters used in the theoretical calculations. Furthermore, the pulsations measured had passed through the lower exosphere and the F_2 ion-density peak, and the filtering action of this region differs somewhat between night and day. Finally, our calculations are based on the assumption of vertical incidence, whereas the observed waves apparently traveled along field lines between conjugate sites and were, therefore, obliquely incident on the ionosphere. One can expect that a circularly polarized Alfvén wave propagating along the field lines toward a middle-latitude ionosphere will break up into an S-wave ($E_y \approx 0$) and an F-wave ($B_y \approx 0$) in the upper ionosphere, producing a mixture of the two types incident on the ionosphere. If so, $|B|_{Ground}$ should have a value somewhere between its values for the incident S- and F-waves.

In any case, we can conclude that daytime collisional absorption does not cause much amplitude attenuation under normal conditions, accounting for a reduction in the transmitted amplitudes by a factor of about 3 at $f \sim 1$ cps. Daytime amplitudes are further reduced by the transformation of part of the incident wave into the highly attenuated e-mode in the lower ionosphere. However, these effects are partly offset by the smaller daytime thickness of the earth--ionosphere cavity, which increases the daytime transmitted amplitudes relative to their nighttime values. The outcome of these competing effects is a day--night amplitude ratio of the order of .5 under near-minimum sunspot conditions. This permits a projection such as that made by Campbell (1967) of ground measurements of the occurrence of pc 1 oscillations and of their frequency variations into the upper ionosphere just below the F_2 peak (at nonpolar latitudes). It is not possible to make a similar projection of ground-polarization measurements at nonpolar latitudes. The fields transmitted through the daytime ionosphere should be predominantly p-mode (right circularly polarized), regardless of the polarization of the incident wave.

Finally, it should be pointed out that although the transmitted amplitude should not undergo large diurnal variations (for a fixed incident amplitude), the fraction of the incident power that is absorbed

may differ significantly between night and day. The fraction of the
incident power absorbed by the ionosphere can be determined from the
elements of the reflection matrix (with a perfectly reflecting earth,
the energy that is not reflected is absorbed by the ionosphere).

While the approximate solutions of the propagation equations
derived in this paper are adequate for the purpose of estimating the
transmission matrix elements, more accurate solutions are needed for
the determination of the reflection matrix elements. These will be
derived in a later paper.

BLANK PAGE

APPENDIX

In order to apply the WKB method to the solution of Eq. (64), it is convenient first to introduce a new variable, u, in terms of which the phase of $q^2(u)$ is constant, except at possible turning points where its sign changes. The variable u and the function $q^2(u)$ for the two forms of $\tilde{v}_i/\tilde{V}_a^2$ are given by

$$u = -\log\left(e^{i\pi/2}\frac{\tilde{v}_i}{\tilde{V}_a^2}\right) = \frac{z}{\zeta_o} - \frac{i\pi}{2} \right\} \tag{A-1}$$

$$q^2_{x,y}(u) = \tilde{u}^2\tilde{\zeta}_o^2\left[\frac{e^u + \frac{1}{\tilde{u}}}{a_{x,y}e^u + \cos\varphi}\right] \tag{A-2}$$

$$\frac{\tilde{v}_j}{\tilde{V}_a} = e^{z/\zeta_o}$$

$$u = \left[e^{i\pi/2}\frac{\tilde{v}_i}{\tilde{V}_a^2}\right]^{-1/2} = \left(1 - \frac{z}{2\zeta_o}\right)e^{-i\pi/4} \right\} \tag{A-3}$$

$$q^2_{x,y}(u) = 4\tilde{u}^2\tilde{\zeta}_o^2 e^{i\pi/2}\left[\frac{u^2 + \frac{1}{\tilde{u}}}{a_{x,y}u^2 + \cos\varphi}\right] \tag{A-4}$$

$$\frac{\tilde{v}_i}{\tilde{V}_a^2} = \frac{1}{\left(1 - \frac{z}{2\zeta_o}\right)^2}$$

where

$$a_x = 1$$

$$a_y = \cos^2\varphi \tag{A-5}$$

We consider the p and e modes separately for both forms of v_i/V_a^2, replacing Eq. (69), in which $\varkappa$ can have either sign, by the following two equations in which the sign of $\varkappa$ is taken to be positive:

$$\mathcal{e}_p''(u) + \underset{px,y}{^2}(u)\mathcal{e}_p(u) = 0 \tag{A-6}$$

$$\mathcal{e}_e''(v) + q_{ex,y}^2(v)\mathcal{e}_e(v) = 0 \tag{A-7}$$

where

$$v = u^* \tag{A-8}$$

$$\mathcal{e}_p(u) = \mathcal{e}(+\tilde{\omega},u) \tag{A-9}$$

$$\mathcal{e}_e(v) = \mathcal{e}^*(-\tilde{\omega},u^*) \tag{A-10}$$

The function $q_p^2(u)$ is given by (A-2) or (A-4), depending upon the functional form of ν_i/V_ε^2.

For $q_e^2(v)$ we have

$$q_e^2(v) = \tilde{\omega}^2\tilde{\zeta}_o^2\left[\frac{e^v - \frac{1}{\tilde{\omega}}}{a_{x,y}e^u + \cos\varphi}\right] \quad \text{for} \quad \frac{\tilde{\nu}_i}{\tilde{V}_a^2} = e^{z/\zeta_o} \tag{A-11}$$

$$q_e^2(v = 4\tilde{\omega}^2\tilde{\zeta}_o^2 e^{-i\pi/2}\left[\frac{v^2 - \frac{1}{\tilde{\omega}}}{\varepsilon_{x,y}v^2 + \cos\varphi}\right] \quad \text{for} \quad \frac{\tilde{\nu}_i}{\tilde{V}_a^2} = \frac{1}{\left(1 - \frac{z}{2\zeta_o}\right)^2} \tag{A-12}$$

For the p-mode, $q_p^2(u)$ has no zeroes, and the application of the WKB method to the solution of (A-6) is straightforward. In applying the boundary condition Eq. (34) at $\tilde{z}_1$, we neglect $1/\sqrt{\tilde{\omega}\tilde{h}}$ as compared to unity. The WKB approximation neglects terms of order $1/\sqrt{\tilde{\omega}\tilde{\zeta}_o}$ as compared to unity, and since $\tilde{h} \sim 10 \tilde{\zeta}_o$, it would be inconsistent to retain terms of the order $1/\sqrt{\tilde{\omega}\tilde{h}}$. Thus, Eq. (34) is replaced by the condition that $d\mathcal{e}/dz$ vanishes at z_1. This gives for $\mathcal{e}_p(u)$

$$\ell_p(u) \approx \frac{2i}{c} [B_x - iB_y \cos \varphi]_{,nc} \exp\left[i \int_{u_o}^{u_1} q_p(u)du\right]$$

$$\times \left[\frac{q_p(u_o)}{q_p(u)}\right]^{1/2} \cos \int_u^{u_1} q_p(u)du \qquad (A-13)$$

where

$$u_o = u(\tilde{z}_o) \qquad (A-14)$$

$$u_1 = u(\tilde{z}_1)$$

For the e-mode, $q_e^2(v)$ has a zero at v_2, where

$$v_2 = \ell n \frac{1}{\omega} \quad \text{for} \quad \frac{\tilde{v}_1}{\tilde{v}_a^2} = e^{z/\zeta_o} \qquad (A-15)$$

$$v_2 = \sqrt{\frac{1}{\omega}} \quad \text{for} \quad \frac{\tilde{v}_1}{\tilde{v}_a^2} = \frac{1}{\left(1 - \frac{z}{2\zeta_o}\right)^2} \qquad (A-16)$$

The WKB method cannot be used near this turning point, but can
be applied for values of v not too near v_2. The usual technique for
solving this type of problem is to replace $q_e^2(v)$ by a linear function
of v near the turning point. The solution of (A-7) when v is near v_2
then becomes a linear combination of Bessel functions of order 1/3:

$$\ell_e(v) = \sqrt{\frac{w}{q_e(v)}} \left[C_1 J_{1/3}(w) + C_2 J_{-1/3}(w)\right] \qquad (A-17)$$

where

$$w = \int_{v_2}^{v} q_\epsilon(v) dv \qquad \text{(A-18)}$$

When $|w|$ is large, the asymptotic form of (A-17) is a linear combination of WKB solutions, so that (A-17) can be used for the whole range of values $z_o \leq z \leq z_1$. We can find C_2 in terms of C_1 by imposing the condition that (A-17) should give a decreasing exponential in the direction away from the turning point towards the region of evanescence. We then use the boundary condition at v_o to determine C_1. The application of this procedure is straightforward, and gives

$$C_2 = C_1 = \sqrt{\frac{\pi \tilde{k}_{x,y} \tilde{\zeta}_o}{6}} \frac{q_\perp}{c} \exp i\left[\int_{v_2}^{v_o} q_e(v) dv - \frac{\pi}{4}\right] (B_x - iB_y \cos \varphi)_{inc}$$

REFERENCES

1. Greifinger, C., and P. Greifinger, "Transmission of Micropulsations Through the Lower Ionosphere," J. Geophys. Res., Vol. 70, May 1, 1965, pp. 2217-2231.

2. Francis, W. E., and R. Karplus, "Hydromagnetic Waves in the Ionosphere," J. Geophys. Res., Vol. 65, November 1960, pp. 3593-3600.

3. Karplus, R., W. E. Francis, and A. J. Dragt, "The Attenuation of Hydromagnetic Waves in the Ionosphere," Planet. Space Sci., Vol. 9, No. 1, 1962, pp. 771-785.

4. Wentworth, R. C., "Maximum Production of hm Emissions, 1," J. Geophys. Res., Vol. 69, July 1, 1964, pp. 2689-2698.

5. Prince, C. E., Jr., and F. X. Bostick, Jr., "Ionospheric Transmission of Transversely Propagated Plane Waves at Micropulsation Frequencies and Theoretical Power Spectrums," J. Geophys. Res., Vol. 69, August 1, 1964, pp. 3213-3234.

6. Field, E. C., and C. Greifinger, "Equatorial Transmission of Geomagnetic Micropulsations Through the Ionosphere and Lower Exosphere," J. Geophys. Res., Vol. 71, July 1, 1966, pp. 3223-3232.

7. Sims, W. E., and F. X. Bostick, Atmospheric Parameters for Four Quiescent Earth Conditions, Electrical Engineering Research Laboratory, University of Texas, Austin, Texas, Report No. 132, September 1, 1963.

8. Campbell, W. H., Low Attenuation of Hydromagnetic Waves in the Ionosphere and Implied Characteristics in the Magnetosphere for PC1 Events, Institutes for Environmental Research Technical Memorandum I.T.S.A.-37, January 1967, Boulder, Colorado.

9. Dawson, J. A., "Comment on the Paper by R. C. Wentworth, 'Evidence for Maximum Production of Hydromagnetic Emissions Above the Afternoon Hemisphere of the Earth,'" J. Geophys. Res., Vol. 72, April 1, 196., p. 2048.

DOCUMENT CONTROL DATA

1 ORIGINATING ACTIVITY	2a. REPORT SECURITY CLASSIFICATION
THE RAND CORPORATION	UNCLASSIFIED
	2b. GROUP

3. REPORT TITLE
MID-LATITUDE VERTICAL TRANSMISSION OF GEOMAGNETIC MICROPULSATIONS THROUGH THE IONOSPHERE

4. AUTHOR(S) (Last name, first name, initial)
Greifinger, Phyllis S.

5. REPORT DATE	6a. TOTAL No. OF PAGES	6b. No. OF REFS.
November 1967	72	9

7. CONTRACT OR GRANT No.	8. ORIGINATOR'S REPORT Nc
DAHC15 67 C 0141	RM-5099-ARPA

9a. AVAILABILITY / LIMITATION NOTICES	9b. SPONSORING AGENCY
DDC-1	Advanced Research Projects Agency

10. ABSTRACT	11. KEY WORDS
A theoretical description of the transmission of extremely low-frequency (below a few cps) geomagnetic waves propagating vertically through the ionosphere at middle and high latitudes, either naturally or as a result of a nuclear burst. The principal findings of the study are: (1) For vertical propagation of frequencies between about .25 and 2 cps at middle latitudes, the order of magnitude of the transmitted magnetic field is insensitive to polarization of the incident wave: changes are not likely to affect it by a factor of more than about 2. (2) The amplitude of the transmitted field decreases exponentially with increasing density of ionospheric ions. (3) Since the relative daytime transmitted amplitudes of the different frequencies are insensitive to changes in ion density, the shape of the amplitude-frequency curve in the upper ionosphere determines the shape at the ground. (4) The day-night amplitude ratio varies between .05 and 1, depending on the ion density; its frequency-dependence is slight for frequencies above about .5 cps. (5) Daytime transmitted fields should be predominantly of right-handed circular polarization, regardless of the polarization of the incident field.	Geomagnetism Atmosphere Wave propagation Nuclear effects Ionosphere